AD-A062 702 GENERAL ELECTRIC CO PHILADELPHIA PA SPACE DIV F/G 10/2
MHD GENERATOR INVESTIGATIONS.(U)
1977 E TATE, B ZAUDERER N00014-73-C-0039
UNCLASSIFIED NL

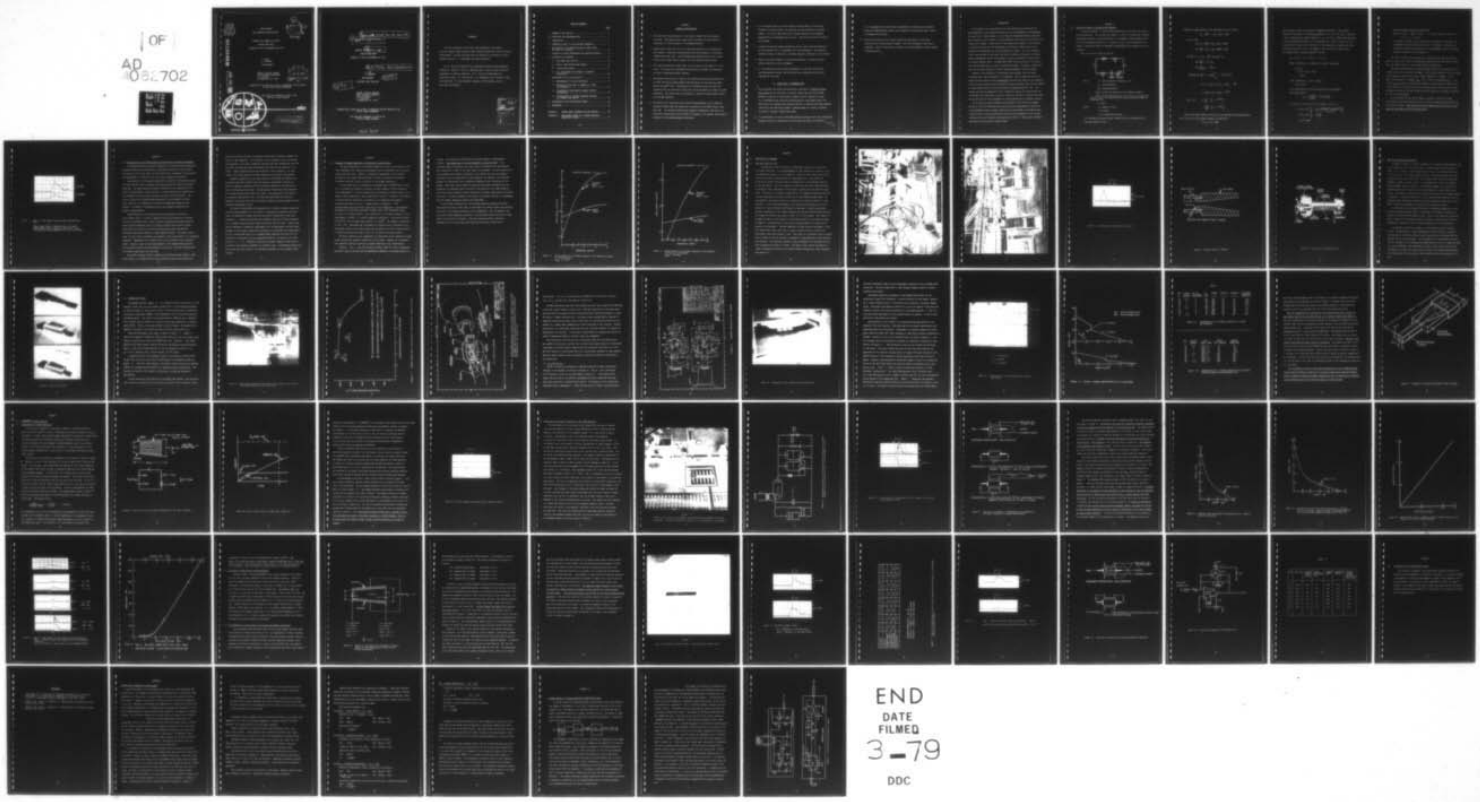

END
DATE FILMED
3-79
DDC

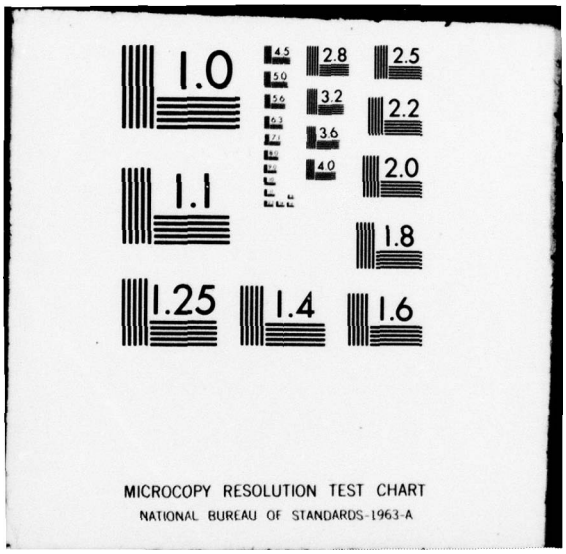
1.0
1.1
1.25
1.4
1.6
1.8
2.0
2.2
2.5
2.8
3.2
3.6
4.0
4.5
5.0
5.6
6.3
MICROCOPY RESOLUTION TEST CHART
NATIONAL BUREAU OF STANDARDS-1963-A

1878 - 1978

(12) SC

LEVEL III

AD32790

ANNUAL REPORT

MHD GENERATOR INVESTIGATIONS

CONTRACT NO. N00014-73-C-0039

PROJECT CODE 9800

OCTOBER 1ST 1976 TO DECEMBER 31ST 1977

E. TATE
B. ZAUDERER

MHD PROGRAMS

GENERAL ELECTRIC COMPANY
SPACE SCIENCES LABORATORY
P.O. BOX 8555
PHILADELPHIA, PA. 19101

THIS WORK WAS SUPPORTED IN PART BY THE
OFFICE OF NAVAL RESEARCH

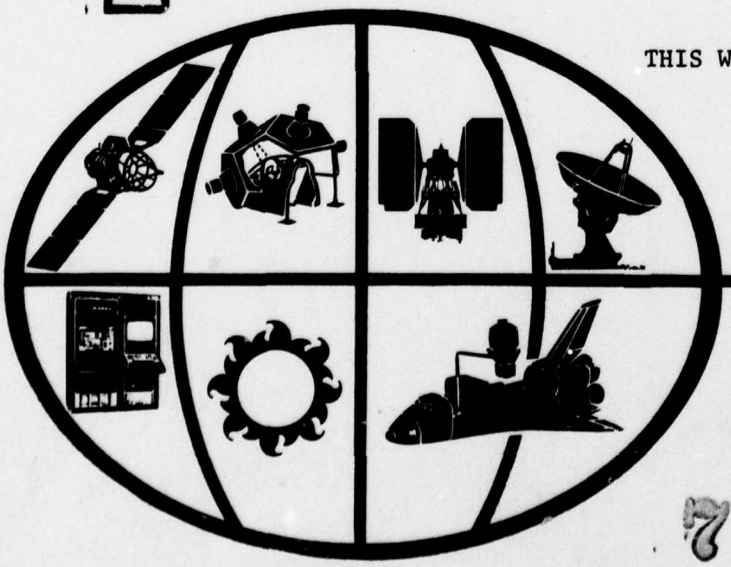

space division SD

78 11 24 031

GENERAL ELECTRIC

(9) ANNUAL REPORT. 1 Oct 76-31 Dec 77,

(6) MHD GENERATOR INVESTIGATIONS.

(15) CONTRACT NO. N00014-73-C-0039

PROJECT CODE 9800

OCTOBER 1ST 1976 TO DECEMBER 31ST 1977

(10) E. Tate Bert Zauderer

E. TATE
B. ZAUDERER

MHD PROGRAMS

TELEPHONE (215) 962-3493

(11) 1977

(12) 76 p.

GENERAL ELECTRIC COMPANY
SPACE SCIENCES LABORATORY
SPACE DIVISION
P.O. BOX 8555
PHILADELPHIA, PA 19101

405 025

THIS WORK WAS SUPPORTED IN PART BY THE OFFICE OF NAVAL RESEARCH

405 025

elt

FOREWORD

The work presented in this report was performed at the General Electric Company, Space Division, Space Sciences Laboratory, King of Prussia, Pennsylvania. The work was done under the auspices of the Office of Naval Research with Mr. J. A. Satkowski as technical monitor.

Mr. E. Tate was responsible for experimental operation and diagnostic evaluation. Messrs. W. Frey, F. McMenamin and G. Fecik provided technical assistance in facility operation. Mr. V. Tilli was responsible for mechanical design. Mr. Tate and Mr. L. D. DeDominicis were technical liason with NASA Ames. Dr. Bert Zauderer, Manager of MHD Programs, was the principal investigator.

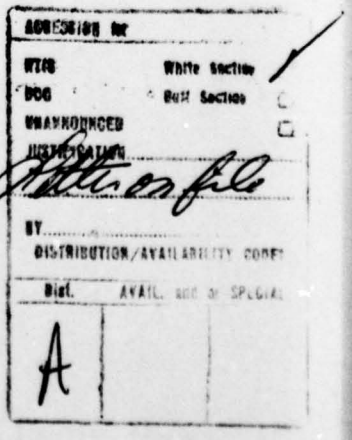

TABLE OF CONTENTS

		Page
1.	SUMMARY OF KEY RESULTS	1
1A.	CONCLUSION AND RECOMMENDATIONS	2
2.	INTRODUCTION	4
3.	THEORETICAL MODEL OF THE BOOTSTRAP GENERATOR	5
4.	CALCULATION OF THE CONDUCTIVITIES OF INERT GASES AND INERT GAS MIXTURES	10
5.	ESTIMATE OF PLASMA TEMPERATURE AND RADIATION COOLING	12
6.	DESCRIPTION OF HARDWARE	16
	6.1 NASA AMES EAST FACILITY	16
	6.2 AMES II SELF-EXCITED MHD CHANNEL	22
	6.3 GE/ONR SHOCK TUNNEL	24
	6.4 GE 1 MHD CHANNEL AND SUMMARY OF PREVIOUS EXPERIMENTS	28
7.	EXPERIMENTS OF THE EAST FACILITY	37
	7.1 MEASUREMENTS OF PLASMA RESISTANCE	37
	7.2 OPERATION OF THE AMES II CHANNEL AS A PURE MHD GENERATOR	42
	7.3 DISCUSSION OF OPEN-CIRCUIT FARADAY VOLTAGE MEASUREMENTS	53
	7.4 INVESTIGATION OF VARIOUS ELECTRODE SURFACES AND CHANNEL AREA RATIOS	53
8.	EXPERIMENTS ON THE GE/ONR SHOCK TUNNEL	64
9.	REFERENCES	65
APPENDIX I	GASEOUS METAL COMPOUNDS FOR MHD SEEDING	66
APPENDIX II	PRELIMINARY DESIGN OF A PLASMA ELECTRICAL CONDUCTIVITY PROBE	70

SECTION 1

SUMMARY OF KEY RESULTS

1. The electrical characteristics of the Ames II channel have been mapped in detail. The maximum power output was 82 kilowatts in argon which is equivalent to a power density of 745 Megawatts/meter^3.

2. Channel area ratios of 2.2:1 to 1:1 have been used and 1.4:1 produced the best results. Electrode configurations with flush surfaces or protruding tungsten pins were used. The protruding pins worked better at low current levels but at large current levels, the flush surfaces worked better.

3. The total electrode arc losses were, for all cases, in the range of 7 to 14 volts. The losses were determined by operating the channel as a generator and also by applying external currents.

4. The deduced conductivity of argon at the maximum operating characteristic of the EAST facility was approximately 800 mhos/meter and the electron number density was $8 \times 10^{17}/cm^3$. Extrapolation of published theoretical data had indicated that the electrical conductivity could possible be as high as 10,000 mhos/meter. The latter level is necessary to obtain kilojoule energy outputs from the MHD generator.

5. Calculations (in conjunction with radiation measurements) of the radiation cooling of argon under the conditions of operation of the EAST facility show that radiation cooling is holding the stagnation temperature (and hence the electrical conductivity) below 13,000 K as opposed to the greater than 18,000 K predicted by the Rankine-Huguenoit equations.

6. It was observed that an initial Farraday voltage (UBD) of 45 volts was necessary for high current, low electrode arc drop operation of the MHD channel. The actual UBD open-circuit voltage induced by the permanent magnet used in the experiment was 12 volts. Thus only low current operation was achieved.

7. A simple theoretical formula giving the current from a bootstrap generator has been devised and is in agreement with the experiments. The generator feedback voltage is treated as a variable negative resistance in this theory.

8. Based on the above results, a self-excited generator to match any given plasma condition can now be designed.

9. It was observed that driven gas contamination in the EAST facility was reducing generator output, and that shock wave attenuation was severely limiting the test time.

1A. CONCLUSIONS - RECOMMENDATIONS

1. The gas dynamic and plasma characteristics achievable in electric driven shock tubes are not sufficient to produce large scale self excited MHD generator operation in noble gases, primarily due to radiation cooling. It is recommended that alternate working gases be investigated and/or the EAST facilty be upgraded with explosive drivers to achieve ultra high pressure, radiatively self-absorbing plasmas, candidate gases are cesium or gaseous or metallic compound, seeded noble gases.

2. The requirements for self excited MHD generator operation have been established, Adequate electrical conductivity and low electrode losses are essential.

Next Page

It is recommended that conductivity improvements be achieved by the methods noted above. (1) Electrode losses can be reduced by either alkali metal coated or impregnated electrodes.

3. Serious discrepancies exist between theory and experiment of electrical conductivities of high pressure plasmas. Also the experimental data base is inadequate. Work in this area is critical to an understanding of these plasmas in MHD generators.

2. INTRODUCTION

This program is an investigation into the production and properties of high temperature, high pressure plasmas and the electromagnetics and gasdynamic interractions of these plasmas in a self-excited magnetohydrodynamic generator. The interactions are strongest in small generators operating with high electrical conductivity plasmas. High pressure, high temperature plasmas can be produced by explosive devices but the experimental difficulties (destruction of the generator and diagnostics on every experiment) are many. For this investigation it was decided to work under less severe conditions (pressures of several hundred atmospheres rather than kilobars) so that the generator would survive for several hundred tests. The NASA Ames "EAST" facility, which is an electrically driven shock-tube, is used to provide the plasma. Presently, (argon test gas) this facility produces a several hundred atmosphere, 13,000 K plasma.

Because of the difficulty of producing these plasmas, there are many questions about their properties to be answered: why are measured electrical conductivities always far below theoretical calculations, what are the electrode losses at large (several hundred amps/cm^3) current densities, what are the effects of large power densities (we have obtained 750 megawatts/$meter^3$), etc. The plasmas can only be produced for short periods of time so the interactions are non-steady, they take time to build up - what are the rates? We have found that the major barrier to the achievement of high temperatures is radiation cooling.

In the past year much progress has been made in this field (see summary - Section 2) and the following areas require further investigation: theoretical and experimental work on plasma conductivities and methods of increasing these conductivities, voltage distributions with particular emphasis on the voltage distribution at the electrode surfaces and the effect of alkali metal seeding on reducing electrode surface voltage losses.

SECTION 3

3.0 Theoretical Model of the Bootstrap Generator

A computer program [1] was developed previously to calculate the current from the generator. This program was complete in that it included the transient MHD generator effects, the multiplication of the magnetic field created by the coil by the permanent magnets, etc. However for day to day operation of the channel a simplified method of checking the experimental data against theory was desirable.

The circuit can be drawn as follows:

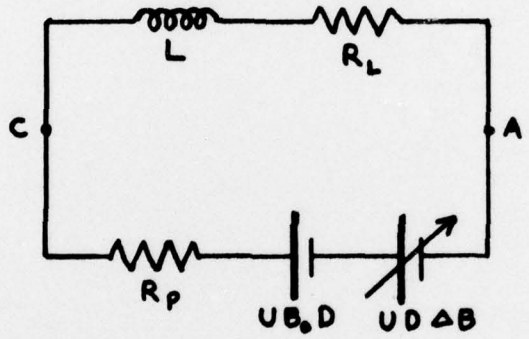

where L = Load Inductance (Bootstrap coil)

R_L = Load Resistance

R_P = Plasma Resistance

UB_oD = Initial voltage due to the permanent magnets

$UB\Delta B$ = The voltage developed as a result of the additional magnetic field (ΔB) created by the current flowing through the bootstrap coil.

$\Delta B = KNI$

where N = number of turns

I = current

K = a calibration constant

K is obtained by passing current through the coil and measuring the resultant magnetic field.

Taking a voltage balance at the electrodes (A and C) gives:

$$IR_l + L\frac{dI}{dt} = -IR_p + UB_oD + UD\Delta B$$

but $\Delta B = KNI$

then $IR_L + L\frac{dI}{dt} = -IR_p + UB_oD + UDKNI$

then $L\frac{dI}{dt} = -IR_L - IR_p + UDKNI + UB_oD$

Putting $R = R_p + R_L - UDKN$ and $UB_oD = E_o$

then $L\frac{dI}{dt} = -RI + E_o$

then $\frac{dI}{I-E_o/R} = -\frac{R}{L}\,dt$

Integrating $\left[\ln (I - E_o/R)\right]_{I_o}^{I} = \left[-{}^{R}/_{L}\,t\right]_{o}^{t}$

$$\ln (I - I_o/R) - \ln (I_o - E_o/R) = -\frac{Rt}{L}$$

$$I - E_o/R = (I_o - E_o/R)\ \ell^{-Rt/L}$$

but $I_o = 0$ $\qquad I = \frac{E_o}{R}\left[1 - \ell^{-Rt/L}\right]$

$$= \frac{UB_oD}{R}\left[1 - \ell^{-Rt/L}\right]$$

This is the same formula as one gets if one ignored bootstrapping except that the R which would appear normally is replaced by

$$R = R_p + R_L - UDKN$$

The bootstrap voltage is replaced by a negative resistance. This formula simplifies the design of a bootstrap generator as it is obvious that to maximize I with a fixed UB_oD one should minimize R. R_L is either an added load resistance or the unavoidable resistance of the bootstrap coil. KN is a function of the bootstrap coil design and it does point out the necessity of knowing the plasma resistance exactly a priori. An example of the use of this formula using the original Ames II design parameters follows:

$R_p = 3.1\ m\Omega$, $R_L = 1.78\ m\Omega$, $L = 1.5\ \mu h$

UDKN = (2000 m/sec) x (.0525 m) x ($.46 \times 10^{-4}$ Tesla/Amp)

= 4.83 mΩ

R = 3.1 + 1.78 - 4.83

= .05 mΩ

UBD = 2000 m/sec x .30 T x .0525 m

= 31.5 Volts

To be conservative a 20 Volt electrode loss was assumed.

The current then is

$$I_{t=\infty} = \frac{31.5-20}{.05\times10^{-3}} = 230 \text{ kiloamps}$$

The current at the end of the test-time ($\simeq$ 1.5 ms) is

$$I = 230 \times 10^3 \left[1 - exp\left(\frac{0.05\times10^{-3} \times 1.5\times10^{-3}}{1.5 \times 10^{-6}}\right)\right]$$

$$= 230 \times 10^3 \left[1 - .9512\right]$$

= 11,224 Amps

The experimentally measured numbers were

UB_oD = 12 Volts, UDKN = 3.7 mΩ, L = 4.0 μh and Rp = 70 mΩ, so

$$R = 70 - 3.7 = 66.3 \text{ m}\Omega$$

R is nearly the same as R_p so the effect of feedback will be small and the maximum current will be $12/66.3 \times 10^{-3} = 180$ amps. This does not include any electrode losses but is in close agreement with the 140 amps actually obtained on run 93 (Figure 4).

One other constraint on the design of a channel is that the time constant given by $L/(R_p + R_L)$ should be approximately the same as the test-time to insure that the current rises to a large value during the test-time.

The above analysis does not include voltage losses at the electrodes but a voltage loss can be subtracted from UBD. As noted later (Section 7.0) the voltage loss is between 7 and 14 volts and is weakly dependent on current. If one uses 10 volts then at 1 kiloamp R_{LOSS} = 10 mΩ and at 10 kiloamps R_{LOSS} = 1 mΩ. To keep R_{LOSS} as small as possible the generator should operate at high current. In any case the loss resistance will be a limiting factor as even with a plasma resistance of zero in the free stream there will always be a residual resistance of 1 mΩ (at 10 kiloamps).

It can be seen that any further gains in current (if one has a large conductivity in the free stream) have to be made by increasing UB_oD and reducing the electrode losses. Reducing the electrode losses and/or their effect on the generator performance will be discussed later.

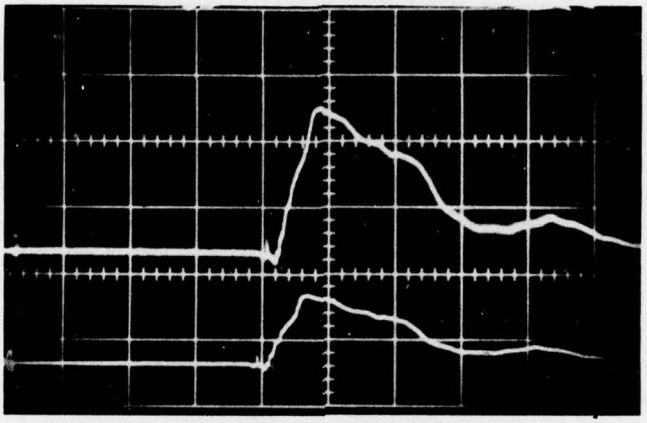

Figure 1. AMES II MHD channel current output into bootstrap coil.

Power output (peak) = 280 watts versus 146 watts output under similar conditions into a 50 mΩ load
The bootstrap current augments the B field by 62 gauss

SECTION 4

4.0 Calculations of the Conductivities of Inert Gases and Inert Gas Mixtures

A literature search was recently conducted to evaluate the most appropriate transport model for the description of equilibrium mixtures of many species. The results of this work, which are described below, culminated in the selection and programming of a model for use in the above computer calculations.

Descriptions of the transport properties of partially ionized gases exploit the small electron mass to separate the heavy particle and electron Boltzmann equations. The heavy particle transport properties can be computed from the theory of Hirschfelder, Curtiss and Bird. For the electrons two approaches to the treatment of the collision operators are taken in the literature. The first is based on the Chapman-Enskog expansion of the Boltzmann or Fokker Plank equations in a complete set of Sonine or generalized Lageurre polynomials. The number of polynomials used in the expansion determines the degree of approximation.

Simplifications of this approach have been proposed in the form of Frost mixture rules. In effect, numerical factors are derived as a function of the Hall parameter which correct transport properties calculated using the weakly ionized Lorentzian limit to values calculated from the exact theory. These models are effective for atoms including Argon where the electron collision cross-section exhibits a sharp Ramsauer minimum. The weakly ionized limit is exact, which circumvents the problem of slow convergence of the polynomial expansion. (Expansions up to twelfth order do not converge in the Lorentzian limit). However, there are two disadvantages to the Chapman-Enskog approach: the correction factors are discontinuous in nature and collision integrals must be evaluated numerically for each case.

The second transport theory is based on the thirteen moment method of Grad which results in a closed form for the distribution function and includes ex-

plicitly the drift velocity, the pressure tensor and the relative thermal flux vector of each component. The advantage of this technique is that the results are expressed in the form of algebraic equations and that integrations over the collision cross-sections need be performed only once for each species of interest. These integrated values are available in the literature. For this reason, this second approach has been selected for the present calculations.

Transport properties for the heavy particles (viscosity and thermal conductivity) have been computed using the method of Hirshfelder, Curtiss and Bird and assuming a Lennard-Jones 6-12 potential applies for interactions between colliding neutral species. Charged species interactions were neglected in the model because their effects are small. The properties of the mixture are computed using Wilke's rule. The above described model has been programmed as sub-routine and trial calculations using the routine agreed well with published experimental values.

The model of Demetriades and Argyropoulos for electron transport properties has also been programmed as a sub-routine. Cross-section integrals which describe the interaction between electrons and neutral species were taken from Reference 2. Coulomb interactions were computed using the collision integrals for a screened coulomb potential taken from Mason, Munn and Smith. These latter results represent a significant improvement over the approximate collision model proposed in the original theoretical development of Demetriades and Argyropoulos. In fact, calculations based on the Chapman-Enskog expansion show that the conductivity as calculated using the approximate model for collisions is in error by 50% at $n = 2.5$. Comparisons between the present computer routine and that of Spencer show excellent agreement for selected cases. Discrepancies between the two results have been traced to the different treatment of the coulombic interactions.

SECTION 5

5.0 Estimate of Plasma Temperature and Radiation Cooling Effects

An actual measurement of the plasma temperature would be both difficult and time consuming as any radiation measurements would be complicated by the contaminants from the driver. However, a temperature measurement is not strictly necessary as the channel MHD performance is directly related to the plasma resistance and hence is very indicative of the plasma temperature.

If the plasma were at a temperature of greater than 17,000°K which it would be in the absence of radiation cooling at the Mach numbers (16-20) involved in these experiments[3] then the argon would be sufficiently ionized (>10%) to not benefit from the addition of small quantities of cesium. To check if the addition of cesium would be beneficial an estimate of the temperature and degree of ionization was made as follows. Figures given in reference 3 show electron density and electrical conductivity versus temperature. The generator resistance of 70 milliohms indicates a conductivity of 857 mhos/metre versus the hoped for 10,000 mhos/metre. The temperature at the channel entrance is thus approximately 12,000°K, or 13,000°K stagnation temperature. The electron density is $8 \times 10^{17}/cm^3$ and the argon number density is 5.5×10^{19}. The degree of ionization is thus 1.45%. This means that the degree of ionization isn't sufficient to get large power outputs but is high enough that the addition of small (≈1%) quantities of cesium would give less than a factor of 2 increase in electron density.

The above estimate of the temperature is conservative as the electrode voltage losses increase the apparent resistivity of the plasma. However, it is apparent that radiation cooling is holding the plasma temperature down significantly.

Figures 2 and 3 show the radiation cooling losses for a two millisecond period for argon at 40 psia and 100 atmospheres compared to the energy density in

the gas. The radiation cooling equals the energy density at approximately 11,500 K. This means that it is very difficult to exceed 11,500 K. The radiation losses calculated do not take account of absorption but nevertheless the calculation is valid at the outer layer of the plasma. The bulk conductivity of the plasma can be high but radiation at the surface can cool the plasma to the extent that the conductivity of the plasma at, for instance, the electrode surfaces is sufficiently low to completely dominate the net resistance of the plasma. This effect can be offset by using pin electrodes protruding into the plasma but, as discussed later, the area of the pins has to be large enough to carry the current otherwise further losses due to current constriction at the pins will occur. The above estimate of the effect of radiation cooling is in agreement with the plasma temperature deduced from experiment.

At very large pressures (e.g. the pressure behind an explosively driven shock wave) the outer cooled layer of the plasma will become thinner and therefore its effect on the plasma resistance will be diminished. Also the magnetic and electrical fields immediately adjacent to the electrode surface will have a large effect on the electron transport. This area requires further theoretical modeling as it is in the range where major self excitation should occur.

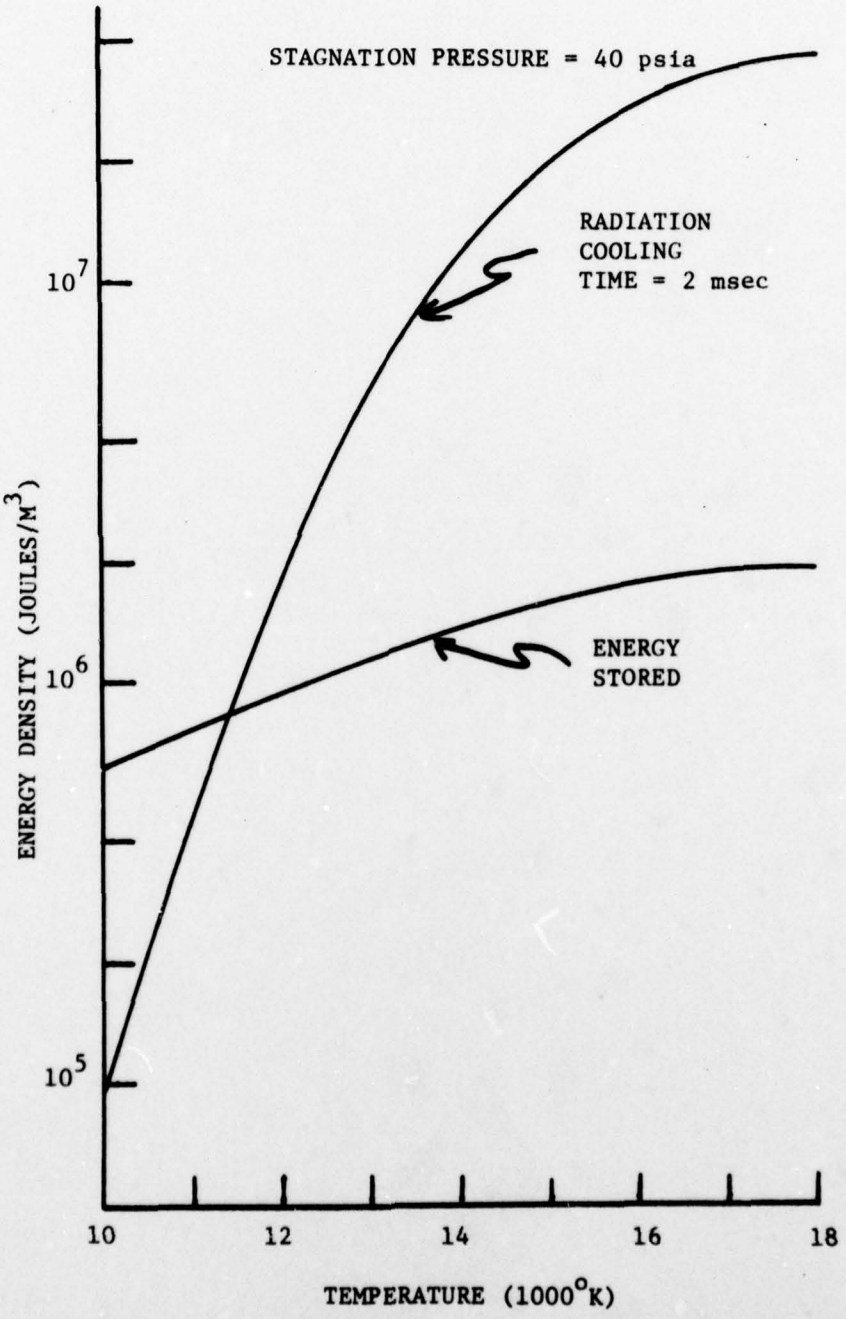

Figure 2. Energy density in the plasma compared to the radiation cooling in 2 milliseconds.
P_{STAG} = 40 psia

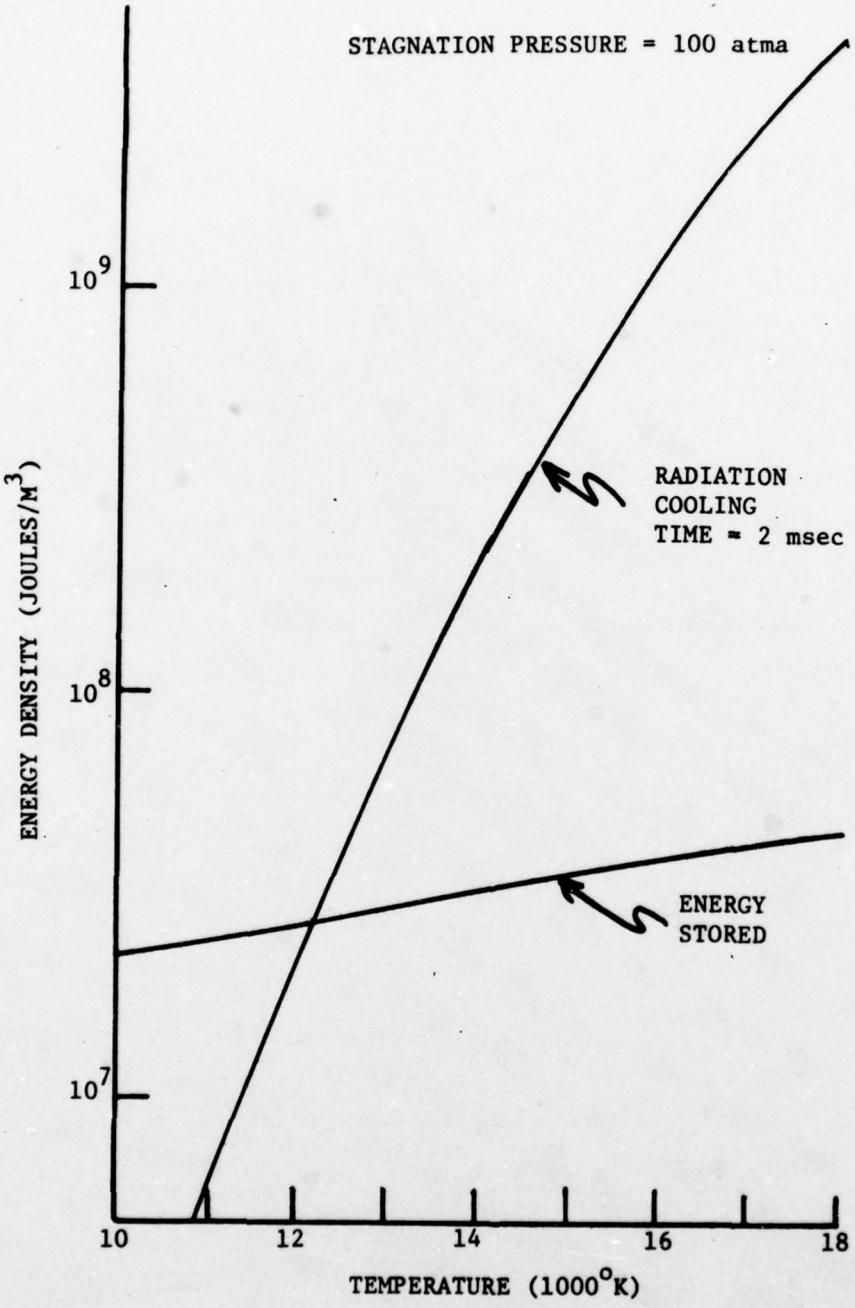

Figure 3. Energy density in the plasma compared to the radiation cooling in 2 milliseconds.
P_{STAG} = 100 atmos

SECTION 6

6.0 DESCRIPTION OF HARDWARE

6.1 NASA Ames EAST Facility

The Nasa Ames "EAST" (Electric Arc Shock-Tube) facility is an electric arc driven shock-tube. It is approximately 45 feet long with a 4 inch I.D. and can withstand pressures of up to 9,000 psi. Figure 4 is an overall view of the facility and Figure 5 shows some of the instrumentation. The facility is versatile as several different driver configurations can be employed depending on the application. The 54" cylindrical driver[2] had previously been identified as giving the best combination of Mach number, pressure and test-time for these tests. The driver arc current is supplied by a 1.2 megajoule capacitor bank and in these experiments the driver current was in the 250-400 kiloamp range. An oscillogram of the driver current on a typical run is shown in Figure 6. Fast response (1 μsec) ionization guages in the driven section measure the time of arrival of a shock and hence the velocity is obtained. Kistler piezoelectric pressure transducers in the sidewall measure the incident shock pressure and also the stagnation pressure (P_5) right in front (1") of the channel. The channel is arranged so that its front face is a reflecting end wall for the shock as shown in Figure 7. Modifications to the facility have been made in the past year to improve its performance. The most important of these was the replacement of the RTV coated driver liner (the liner is shown in Figure 8) with a "Delrin" (a proprietary alkyd resin plastic) liner. This liner is a necessary driver insulator and is exposed to the arc and hence is exposed to high-temperature, high pressure deterioration. Any insulator exposed to this environment will decompose and the chief decomposition product is carbon. The Delrin liner reduced the amount of carbon contamination and hence the channel's MHD performance was vastly improved (see Section 7).

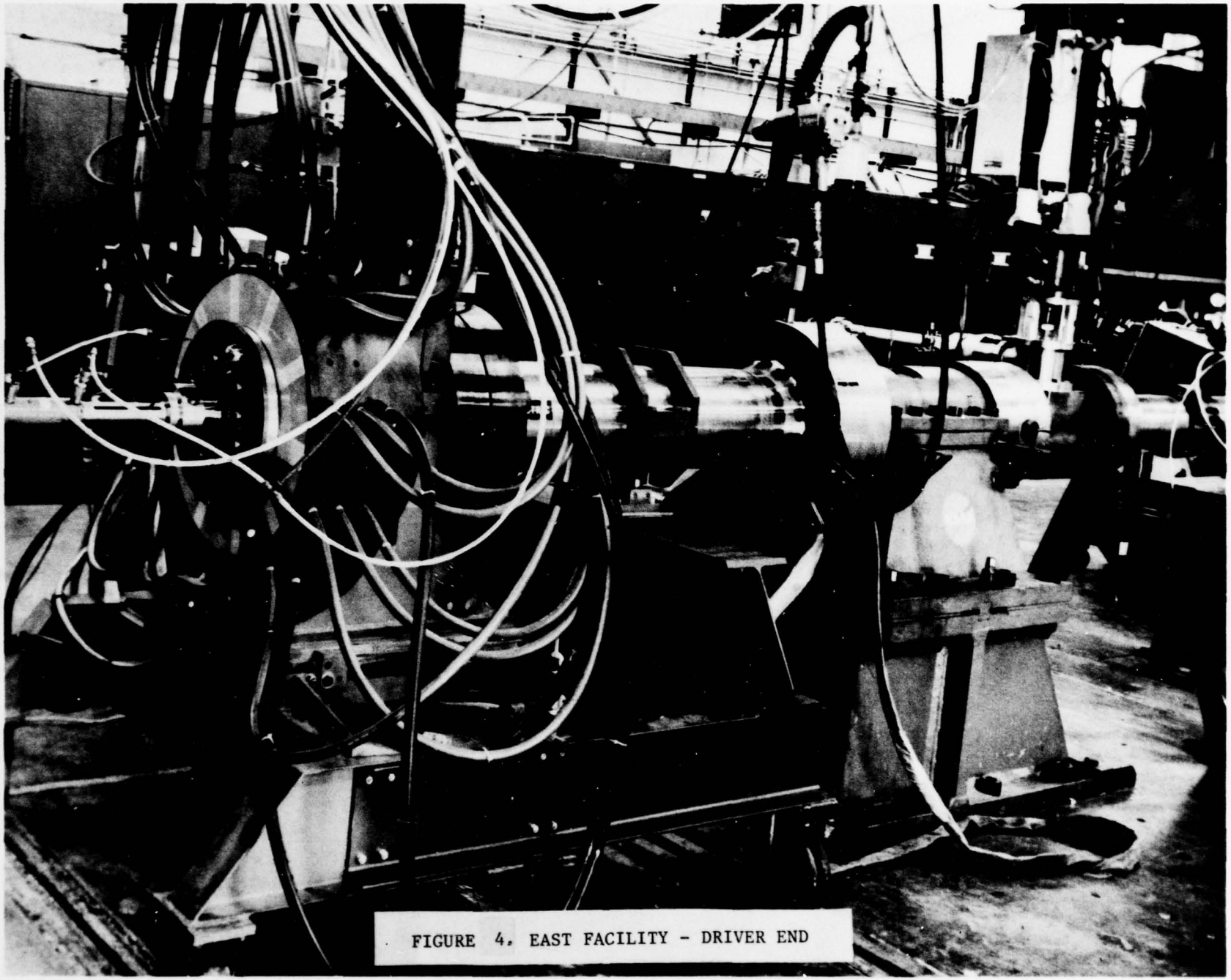

FIGURE 4. EAST FACILITY - DRIVER END

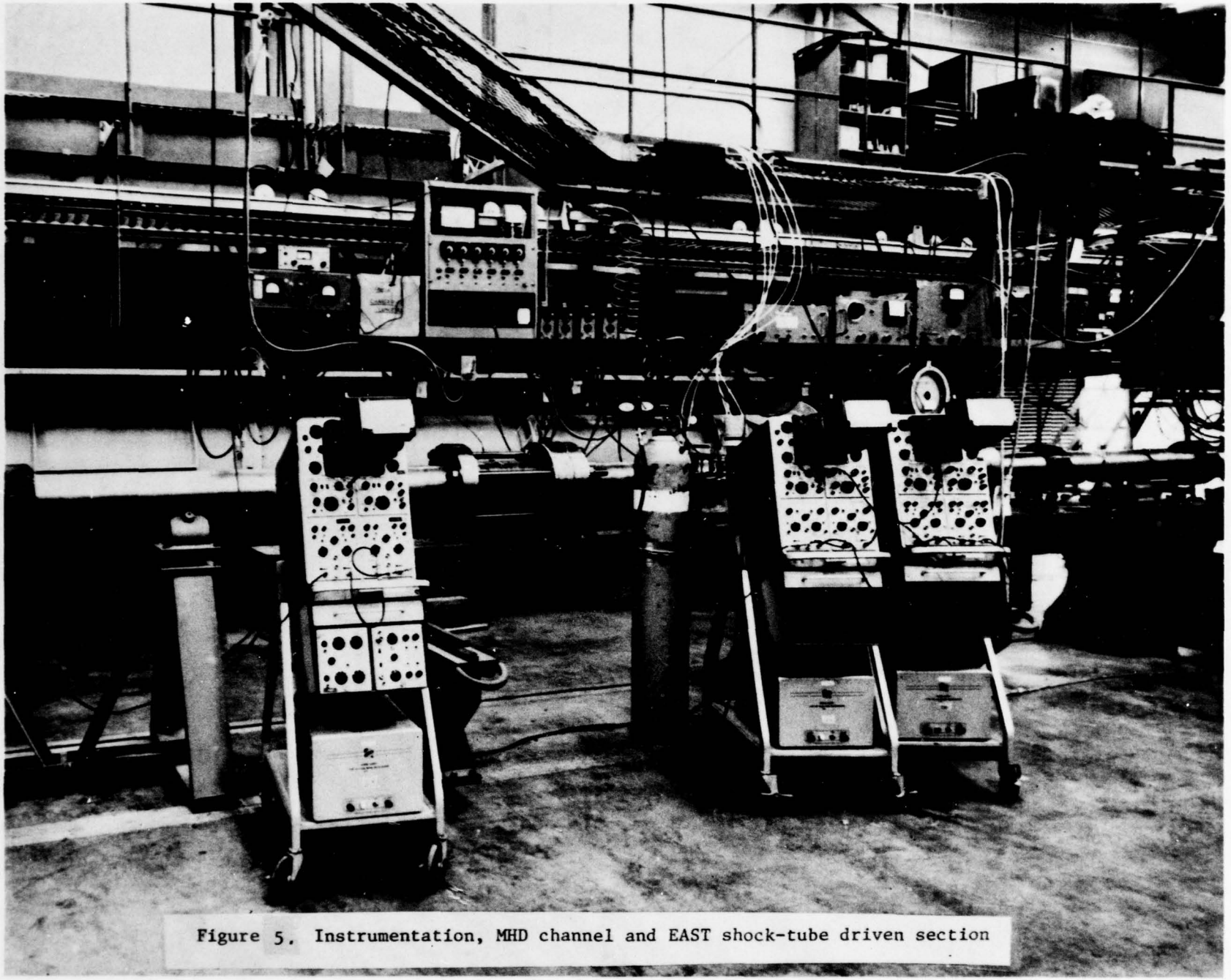

Figure 5. Instrumentation, MHD channel and EAST shock-tube driven section

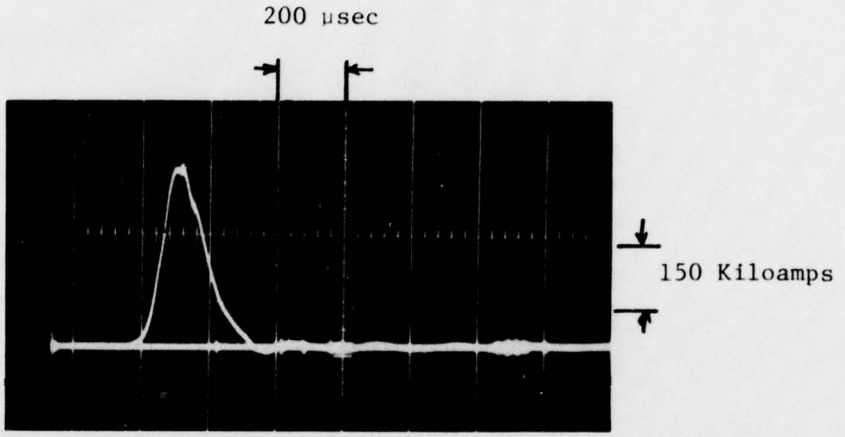

Figure 6. Oscillogram of the EAST Driver Current.

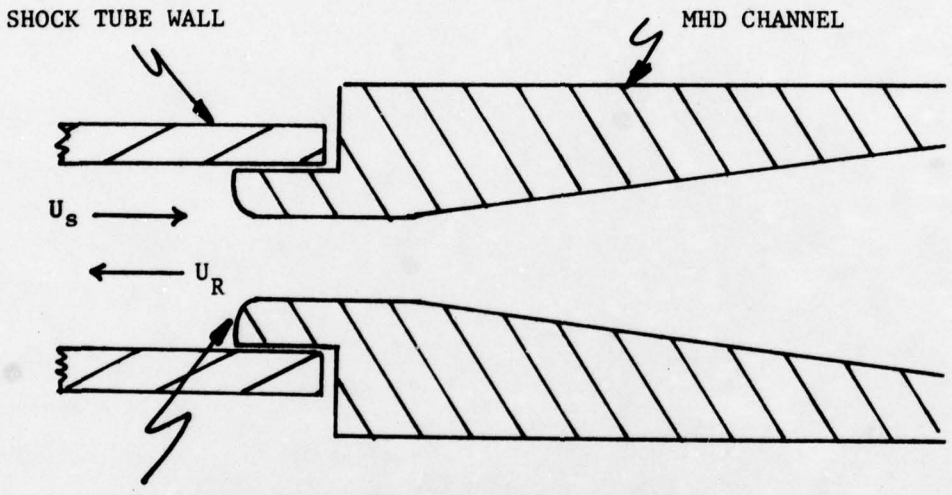

Figure 7. Channel (Ames II) Schematic

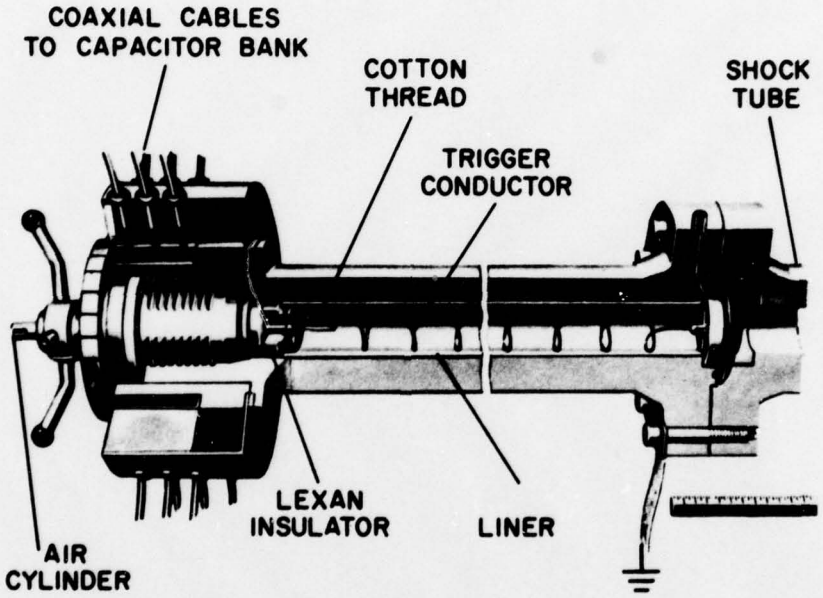

Figure 8. Electric Arc Shock-Tunnel Driver

6.2 Ames II Self-Excited MHD Channel

The Ames II channel is similar to Ames I[1] in internal channel geometry but with a larger outlet to inlet area ratio to offset the gas deceleration as a result of J x B forces. The entrance area is 3.5 cm x 1 cm and the exit area is 7.0 cm x 1 cm. The overall length is 16 cm. The inside surfaces are boron nitride with two copper electrodes. The internal boron nitride and electrode assembly is shown in Figure 9 (Top). This assembly fits inside the permanent magnet assembly, Figure 9 (Center). The permanent magnet is fabricated from samarium-cobalt and is laminated (with epoxy bonding) to reduce eddy current losses. This magnet provides a field in the active region of the channel uniform to within 2%. A field of between 0.2 and 0.3 Tesla had been hoped for but the necessary epoxy bonding and supporting structure reduced the gap field to 0.14 Tesla. There are two magnets, one above and one below the channel.

A coil having 2 turns wrapped around the top permanent magnet and 2 turns around the bottom permanent magnet is connected to the channel electrodes to provide the self-excitation magnetic field. The coil was fabricated using Litz wire to reduce its AC resistance, Figure 9 (bottom). Holes are drilled in the wrapping for connection of the coil and electrodes and for instrumentation.

The channel construction results in a large leak rate (hence impurity level). The channel has a copper diaphragm at its back surface to separate the test gas in the driven section from the dump tank so any leakage from the channel will be in the test-gas. As the channel has to be removed after every run for cleaning a front diaphragm was deemed practical and so a change was made to a front diaphragm. This separates the channel leak from the test gas and considerably increases the purity level as roughly five minutes passes between the introduction of the test gas to the driven section and the completion of a run.

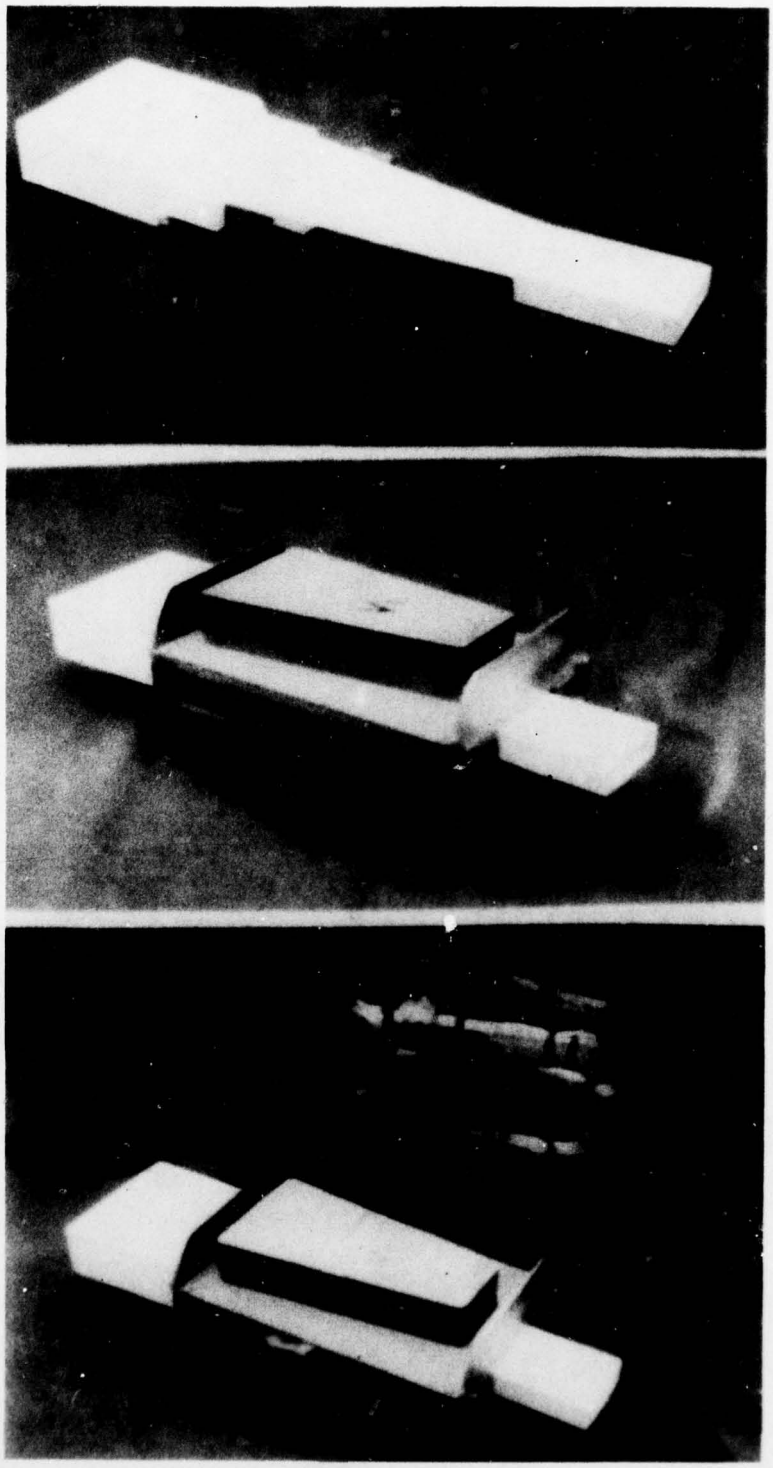

Figure 9. Ames II MHD Channel

6.3 ONR/GE Shock Tunnel

The ONR/GE facility, Figure 10 is a reflected shock tunnel with a 6 inch diameter driver and a 12 inch diameter driven tube. It was designed primarily to deliver plasma for testing up to 10 ms at the relatively modest temperature and pressure (typically 3500°K, 5 atm) appropriate for a non-equilibrium, noble gas MHD generator. The driver can be pressurized to 2500 psi and is equipped with external electric heaters to raise the driver gas temperature to approximately 600°K. These are the upper bounds on driver energy. Performance then depends on the gas in the driven tube and the driven tube pressure p_1.

Predicted performance with argon is shown in Figure 11. Figure 11 shows that stagnation temperature drops rapidly above p_5=5 atm so an upper bound reference condition was taken as 12,000°K and 5 atm. Figure 11 also shows measured shock Mach numbers obtained during the preliminary testing discussed later. A test time of approximately 1.5 ms was obtained at the M_s = 7.6, p_1 = 5 torr condition with a channel having a 50 cm^2 throat.

A capacitor powered electromagnet capable of delivering a uniform field of more than 3 Tesla for more than 10 milliseconds is available, as shown in Figure 12. With this electromagnet, any desired initial field can be applied without the encumbrance (and expense) of a permanent magnet installation. The facility is therefore well suited to exploratory testing and diagnostic measurements.

Initial experiments were done with an available MHD channel to get the test-time stagnation temperature (T_5) and stagnation pressure (P_5) capability of the

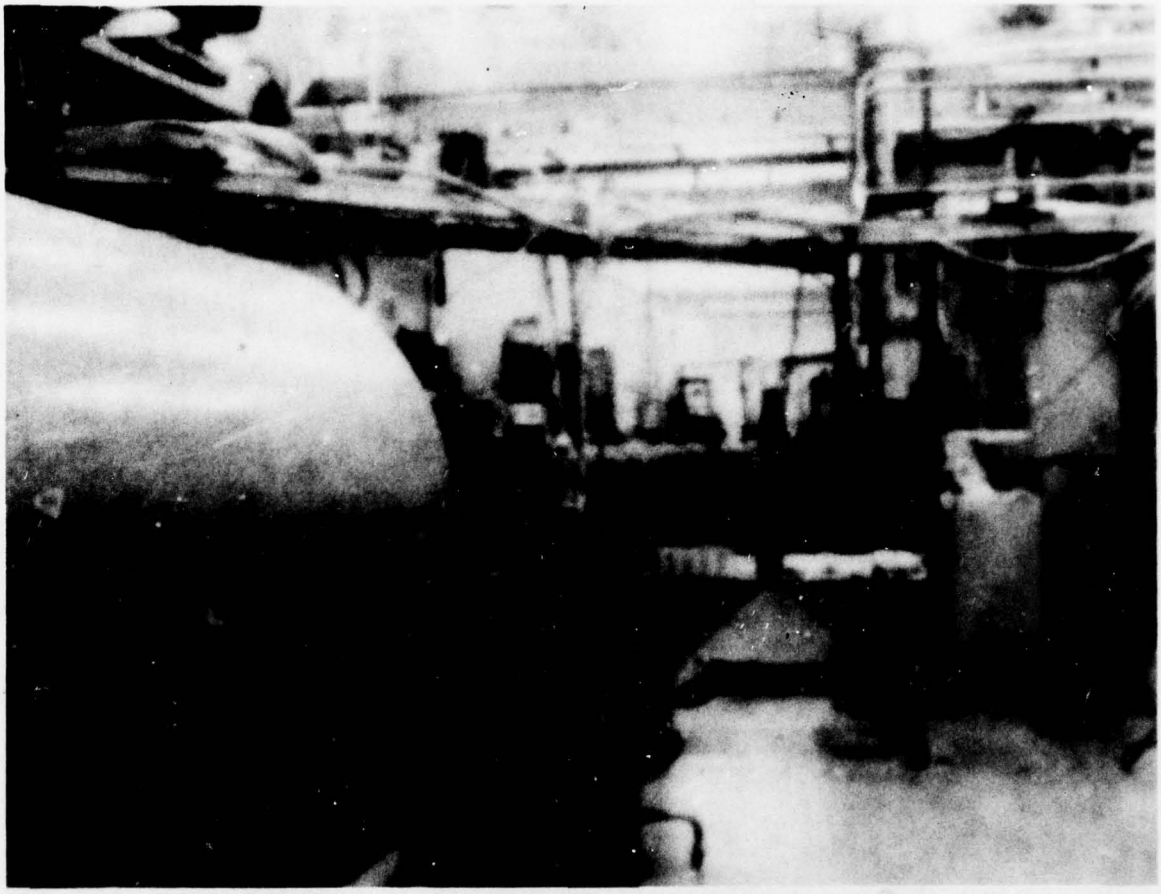

Figure 10. ONR/GE Shock Tunnel Facility showing the Driver at the Far End and an MHD Generator at the Front, left.

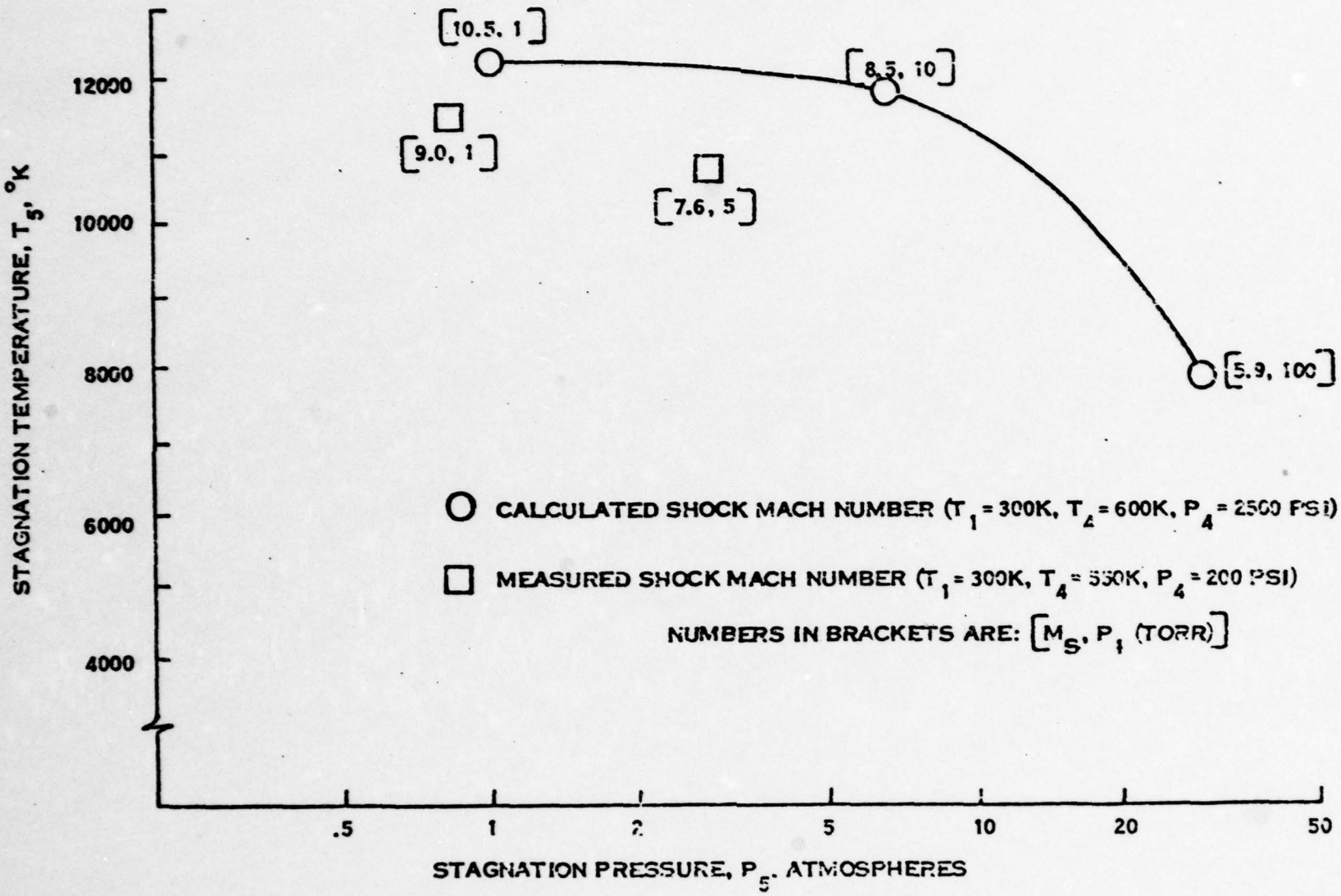

Figure 11. ONR/GE Shock Tunnel Performance, Helium Driver, Argon Test Gas.

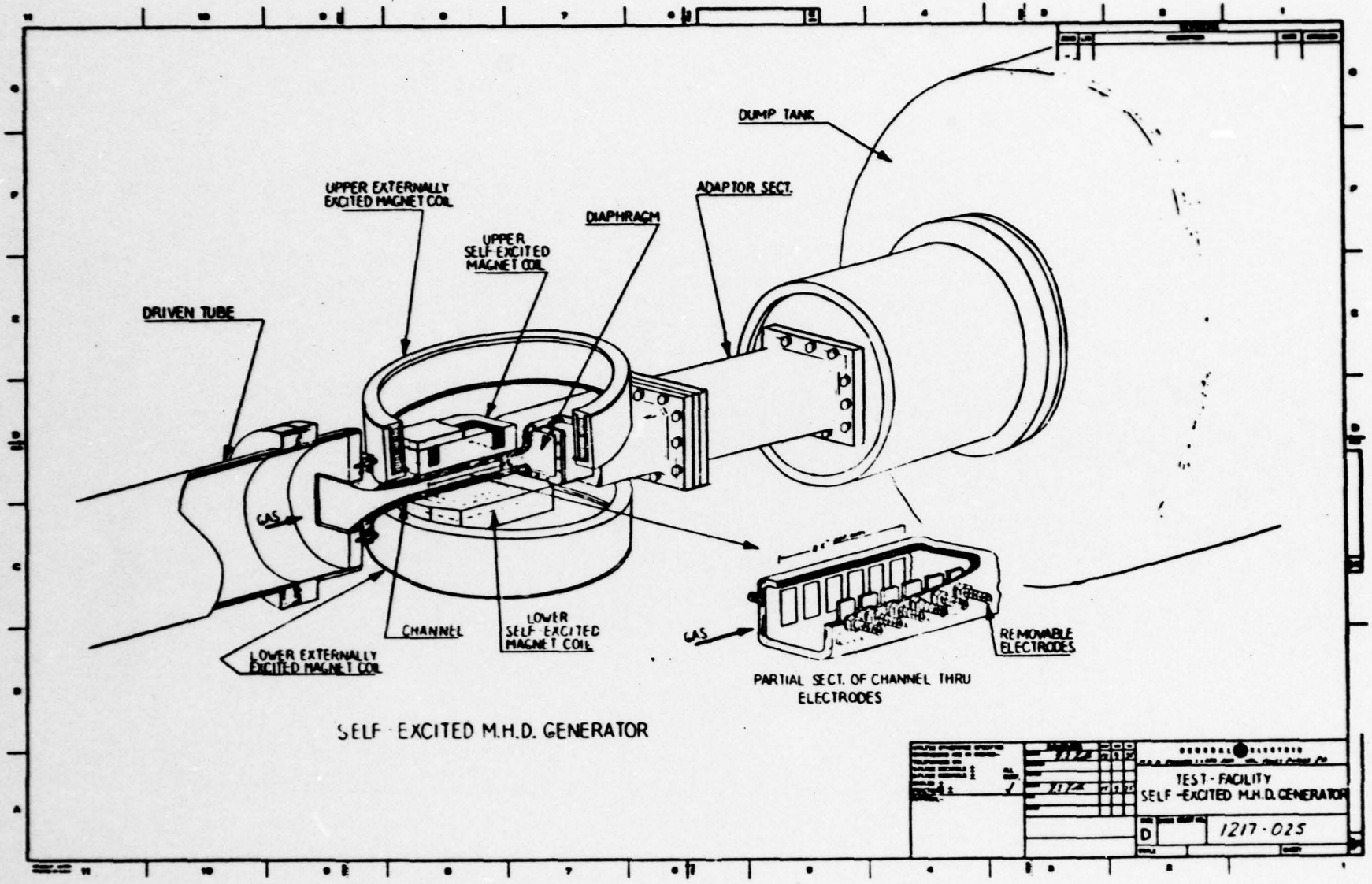

Figure 12. Early PSEMG Diagnostic Channel Concept showing Installation in ONR/GE Shock Tunnel with Externally Powered Magnet Coil to Supply the Initial Magnetic Field (for Actual Channel Configuration, see Figure 5.8).

shock-tunnel. At a P_1 of 5 mm Hg and P_4 of 1200 psia the test-time, T_5 and P_5 were 1.5 ms, 10,600°K and 2 atmospheres respectively.

The MHD experiments done with this channel have been fully reported in Reference 1 and only a brief summary is given here. The Hall parameter was less than unity and the channel was operated with all electrode leads connected externally to give, in effect, a single electrode pair. The power output dropped 40% as compared to segmented electrode operation, which proved that the experimental conditions were already in a regime where segmentation of the electrodes is not critical. Channel construction is considerably simplified with the corollary benefits of simplified measurements and analysis. In the Ames II experiments the pressure was nearly two orders of magnitude higher so the Hall effect was negligible.

The conclusions from this series of experiments were that the shock tunnel was capable of producing a plasma with a conductivity large enough to do meaningful high magnetic Reynolds numbers experiments with sufficient test time (~1.5 ms). The next channel to be described (GE I) was specifically designed for high magnetic Reynolds number operation and its geometry tailored to conditions achievable in the shock-tube.

6.4 GE I MHD Channel

The GE I channel was designed to study MHD operation at high temperatures. Drawings of the assembly are shown in Figures 12 and 13 and a photograph of the channel in place on the shock-tube in Figure 14. The channel has a throat size of 5 cm x 8 cm and has a divergence such as to keep the flow subsonic when operating at designed power output. The geometry of the channel was described fully in Reference 1. There are five pairs of copper electrodes which

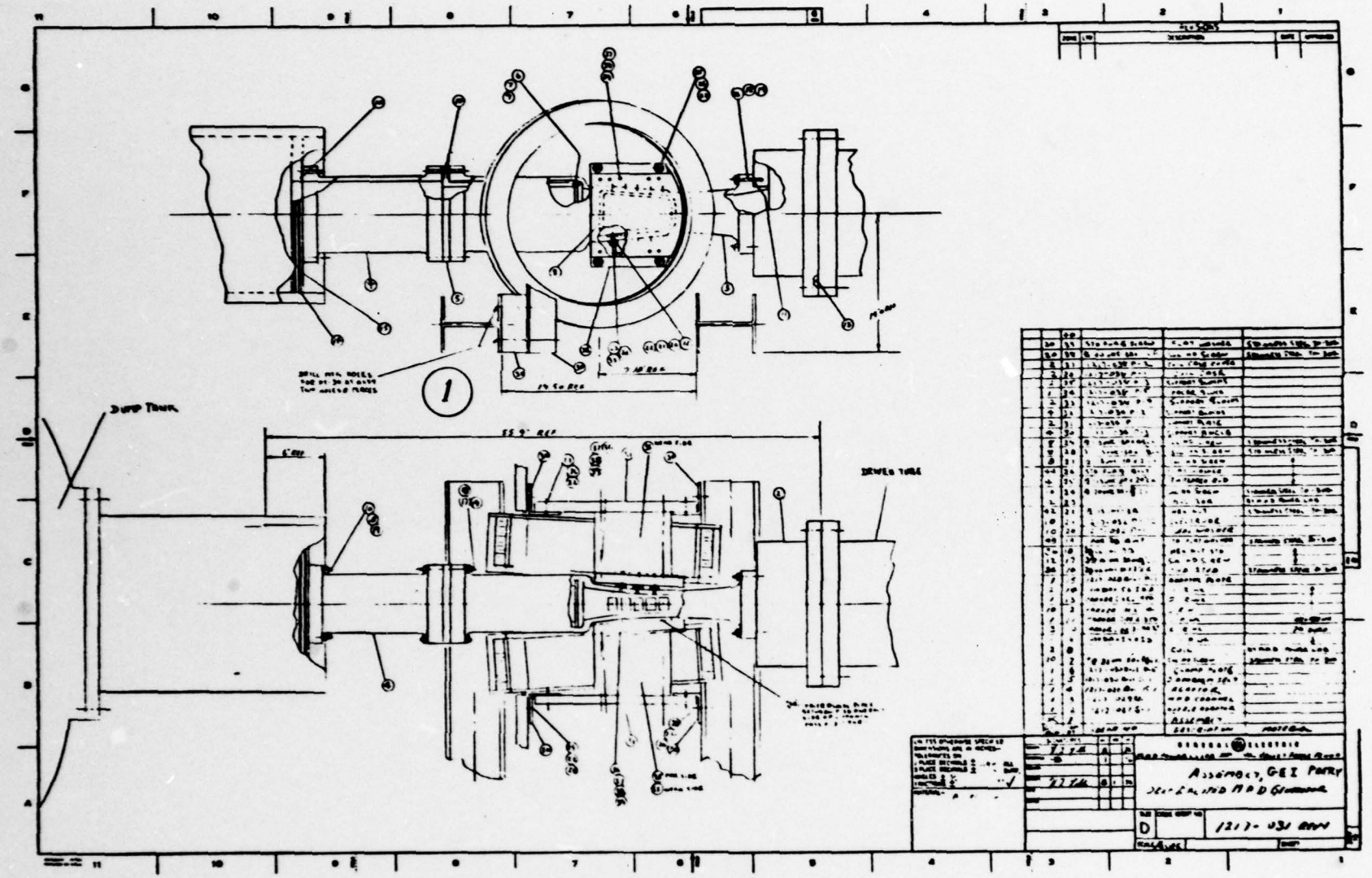

Figure 13. Assembly Drawing of GE I Channel.

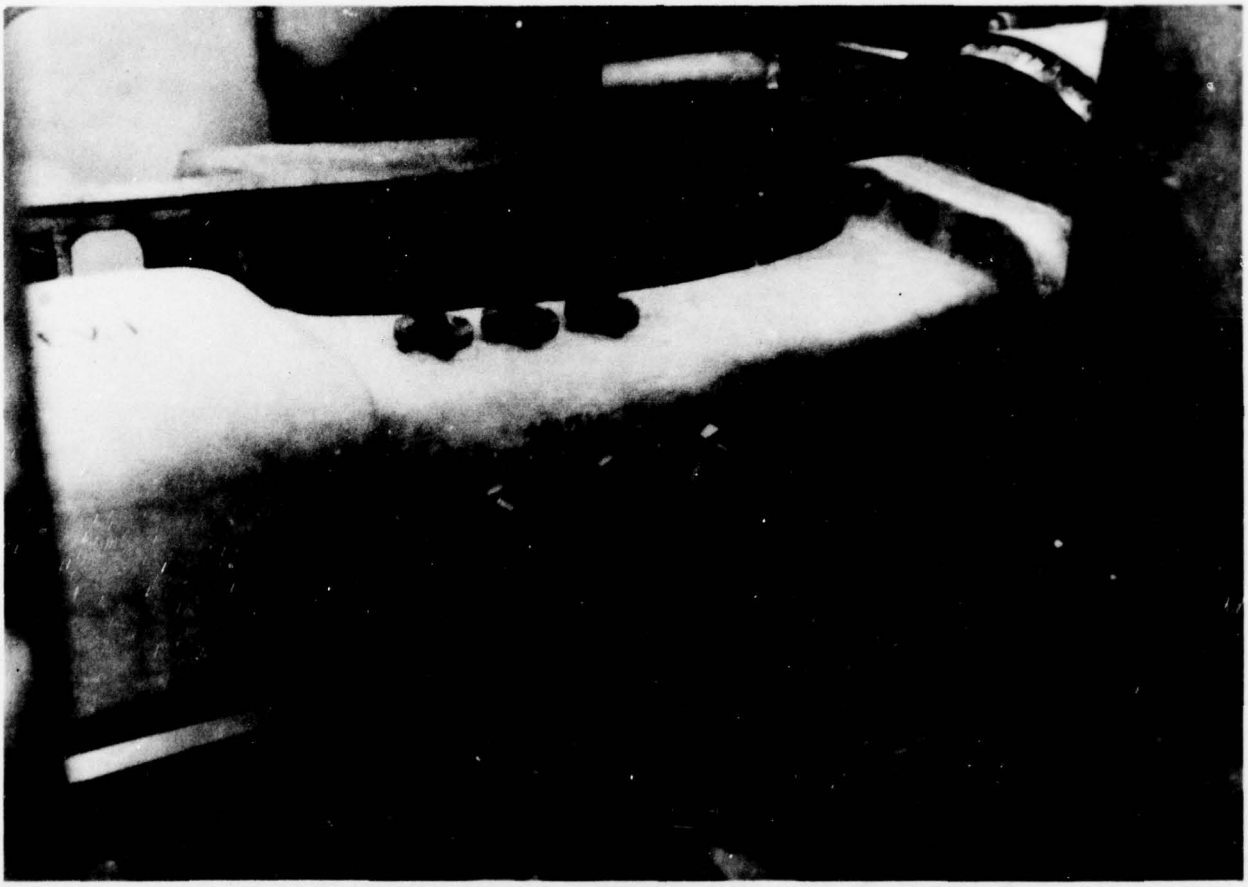

Figure 14. Photograph of GE I Channel during Installation

can have individual loads or can be externally connected to form a single electrode pair. The five anodes have a .005" sprayed tungsten surface to reduce oxidation and erosion.

The plasma conditions achievable in the GE/ONR shock-tunnel are not sufficient to give full excitation. A split-solenoid air-core magnet, powered by a 2 farad capacitor bank, is therefore used to simulate a permanent magnet field. This gives experimental flexibility to pick the magnetic field and also freedom to explore the channel operation as a pure MHD generator. A coil for self-excitation experiments is also placed around the channel. It has 3 turns above and 3 turns below the channel.

The operation of this channel in a standard Faraday MHD generator configuration has been explored. Some shorting of the current downstream at the diaphragm holder was experienced. Replacement of aluminum flanges with fiberglass reinforced epoxy and teflon spraying of other metal surfaces minimized the problem. Current at four of the electrode pairs are shown on Figure 15 and the voltage-current characteristics obtained are compared to theoretical calculations on Figure 16 . The theoretical curves do not include any electrode or end losses. The power outputs obtained are thus very good although the magnitudes of the apparent voltage losses are higher than past experience with General Electric's low temperature Faraday generators would have led one to expect. However, this generator's interaction length is only 15 cm versus the 120 cm of the GE ST-40W channel and thus end effects undoubtedly play a much greater role. Table 1 presents results of generator operation in three different configurations - (a) simple MHD generator with 5 electrode pairs (b) simple MHD generator with a single electrode pair and (c) with the generator output applied to the augmenting coil. Table 1 shows that the enthalpy extraction (electrical power out/heat in) varies from 0.9% at 0.5 Tesla to 11.5% at 1.3 Tesla. The highest enthalpy extraction obtained from the ST-40W channel

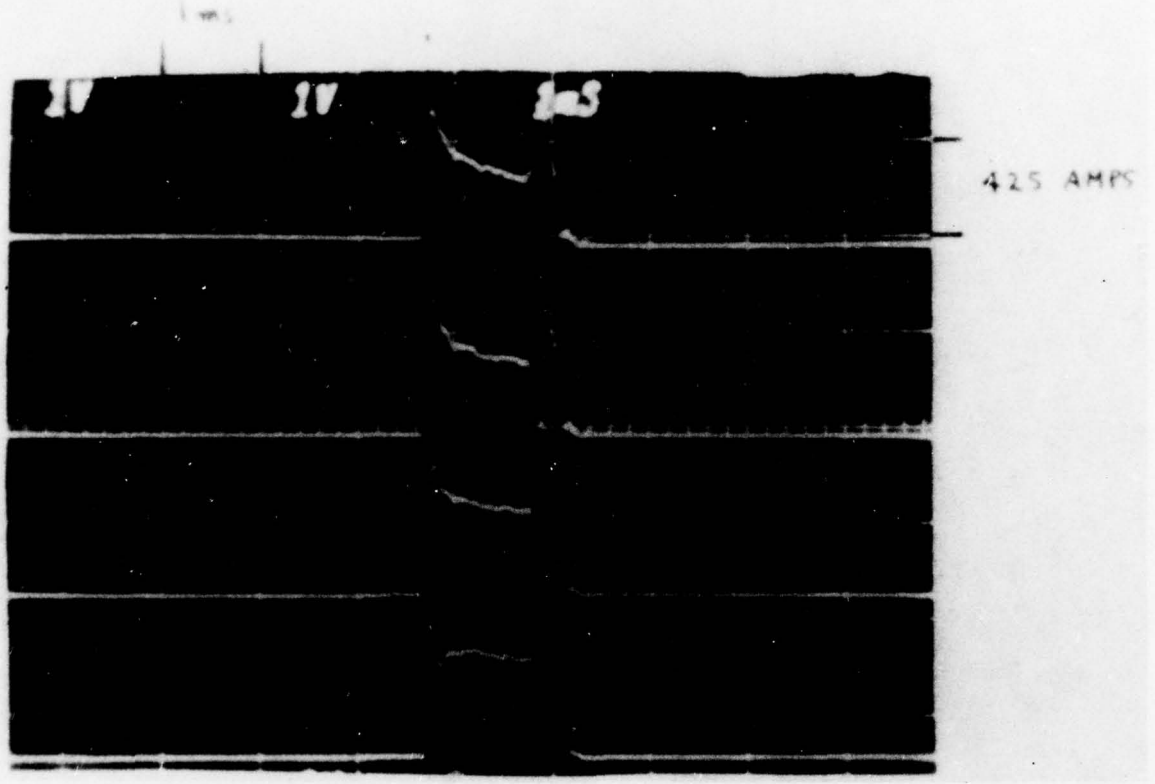

P_5 = 2 atmospheres

T_5 = 10.600°K

B = 1.35 TESLA

Figure 15. Currents from 4 of the Electrodes in the GEI MHD Channel

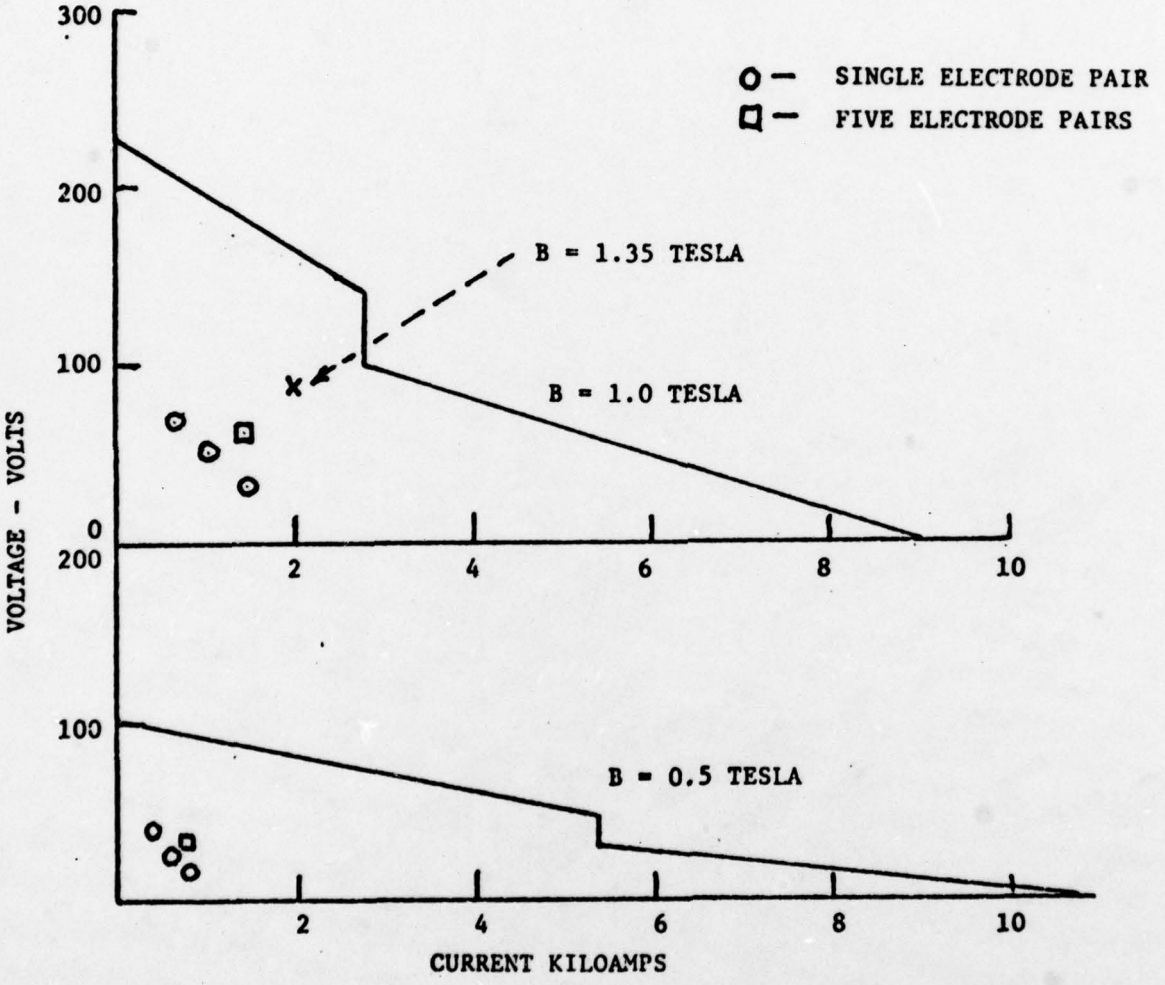

FIGURE 16. VOLTAGE - CURRENT CHARACTERISTICS OF GE I MHD CHANNEL.

TABLE 1

RUN	B FIELD (TESLA)	NO. OF ELECTRODES	R_L (mΩ)	I(AMPS)	V(VOLTS)	POWER(KW)	% ENTHALPY EXTRACTION
30	0.5	1	100	400	40	16	1.0
25	"	1	46	600	25	15	0.93
28	"	1	22	800	18	14	0.87
17	"	5	46	725	33	24	1.5
31	1.0	1	100	1125	70	49	3.1
20	"	1	46	600	52	58	3.6
29	"	1	22	800	33	49	3.1
15	"	5	46	1450	67	97	6.1
18	1.35	5	46	2000	92	185	11.6

TABLE 1(a) PERFORMANCE OF GE I CHANNEL OPERATING AS A SIMPLE MHD GENERATOR

RUN	B FIELD (TESLA)	LOAD (COIL + xmΩ)	ENERGY OUT + (JOULES)	AVERAGE POWER (KW)
33	0.5	COIL + 0	34	22
39	"	COIL + 2	41	32
36	"	COIL + 3	56	36.5
41	"	COIL + 10	61	44.5
34	1.0	COIL + 0	160	114
38	"	COIL + 2	165	120
37	"	COIL + 3	214	153
42	"	COIL + 10	183	131
35	1.35	COIL + 0	228	163

TABLE 1(b) PERFORMANCE OF GE I CHANNEL OPERATING WITH THE POWER OUTPUT DELIVERED TO THE AUGMENTING COIL

was 19% at the much higher field of 2.8 Tesla, so in terms of enthalpy extraction, this generator is performing in excellent fashion. The power output went down during single electrode pair operation by 40-50% compared to 5 electrode pair operation (this is in agreement with the results discussed previously).

With the augmenting coil connected to the electrodes more power (using the same plasma conditions) was obtained than in the simple Faraday mode (Table 1). This was a combination of (a) better matching of the generator impedance to the external load, and (b) the generator current applied to the coil gave an effective 7→8% increment in B. A resistor was in series with the coil for the results presented in Table 1 to give better load matching. The average power for Run 36 was 35 K watts and the output energy was 56 joules. This particular case is for the lowest B field used (0.5 Tesla) and as can be seen from Table 1 the power (and energy) output goes up nearly exactly as B squared. The emphasis has been on low B field because a self-contained PSEMG would be restricted to the magnetic fields obtainable from permanent magnets. However the power output at higher B fields is of interest as it shows what power levels would be reached if greater augmentation was achievable. So far the power output goes up as B squared with no levelling off, i.e. end shorting or any other loss mechanism present is not becoming more important as B increases.

The conclusions, thus far, from these experiments are that the MHD generator self-excitation concept is sound but, of course, plasma energy densities several orders of magnitude larger and plasma temperatures twice as large will be required to give energy outputs in the kilojoule range in a small package.

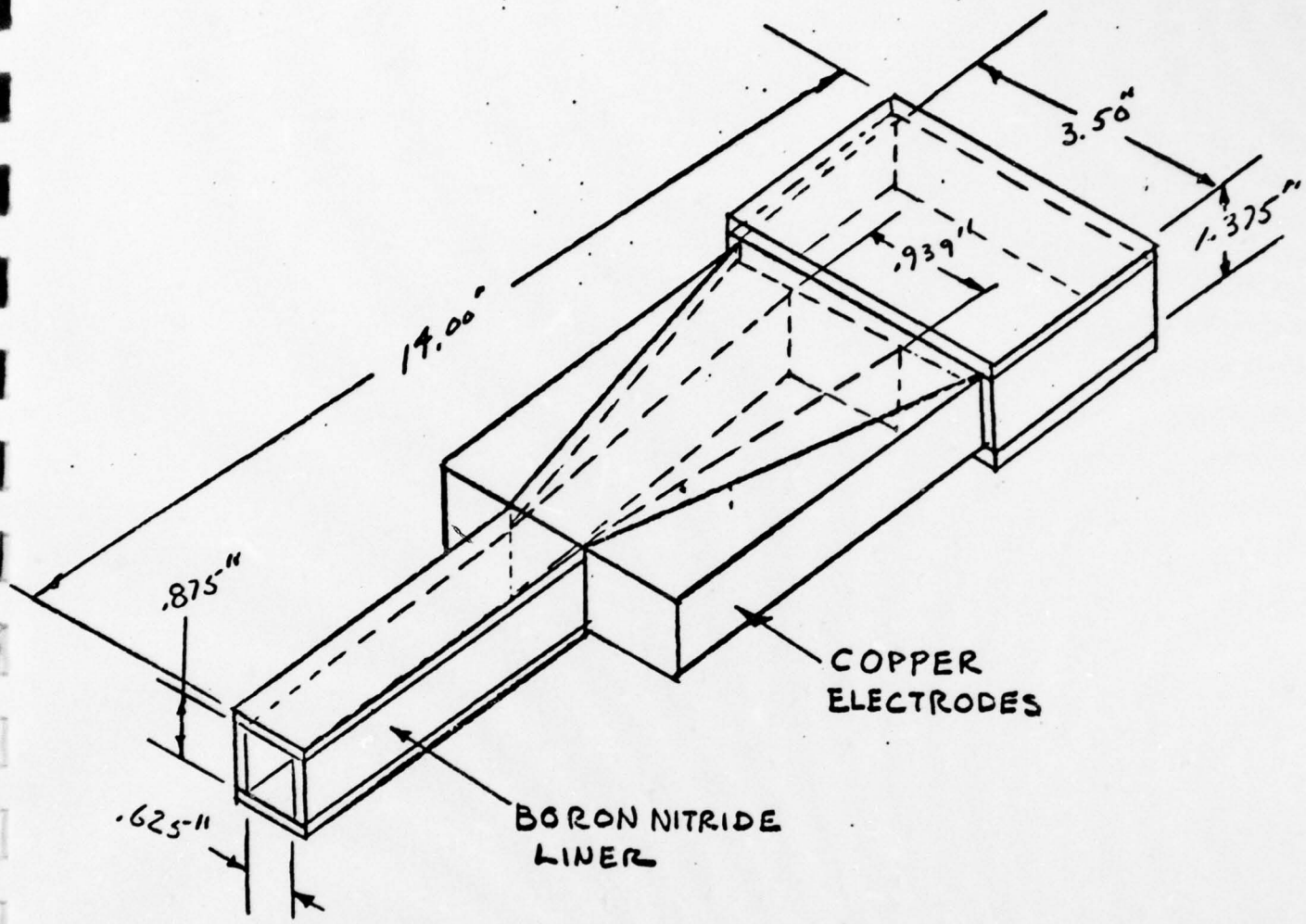

Figure 17 . Schematic of Interior Construction of Ames I Channel

SECTION 7

7.0 EXPERIMENTS ON EAST FACILITY

7.1 Measurements of Plasma Resistance

As the initial operation of the Ames II channel in bootstrap operation gave very little output[3], a series of experiments were done to measure the plasma resistance. A higher than expected plasma resistance (low electrical conductivity) will have dramatically deliterious effects upon bootstrap operation as the channel aerodynamic and electromagnetic design parameters have to be tailored exactly to the plasma resistance (and test-time). A brief description of the channel design considerations (as they relate to the plasma resistance and test-time) follows.

The electrical and geometrical parameters of the channel are shown in Figure 18. There are 2 turns of the bootstrap coil on top in series with 2 turns on the bottom. The L/R_{TOTAL} ratio determines the rise-time of the current generated by the channel (the initial voltage is supplied by UBD with the B field supplied by the permanent magnet). If this ratio is too large, then a current output similar to that shown in Figure 19(large L/R) results. The current rises slowly and doesn't reach an appreciable value by the end of the test-time. If the L/R ratio is too small then the current rises quickly but to a low value as obviously a large R limits the output of the generator. An L/R of approximately the same value as the plasma test-time is needed. The design numbers shown on Figure 18 were for an expected test-time of 1-1½ milliseconds and a plasma resistance of 3 milliohms. The design L/R was

$$\frac{L_{COIL}}{R_{PLASMA} + R_{COIL}} = \frac{4.0\ \mu h}{4.0\ m\Omega} = 1 \text{ millisec}$$

The resistance of the coil is unavoidable but was minimized by using "Litz" wire to keep its AC resistance small. A further degradation of the generator output (as a result of a larger than expected plasma resistance) occurs as a result of the design area ratio. An area ratio of 2.1 was chosen on the basis of an

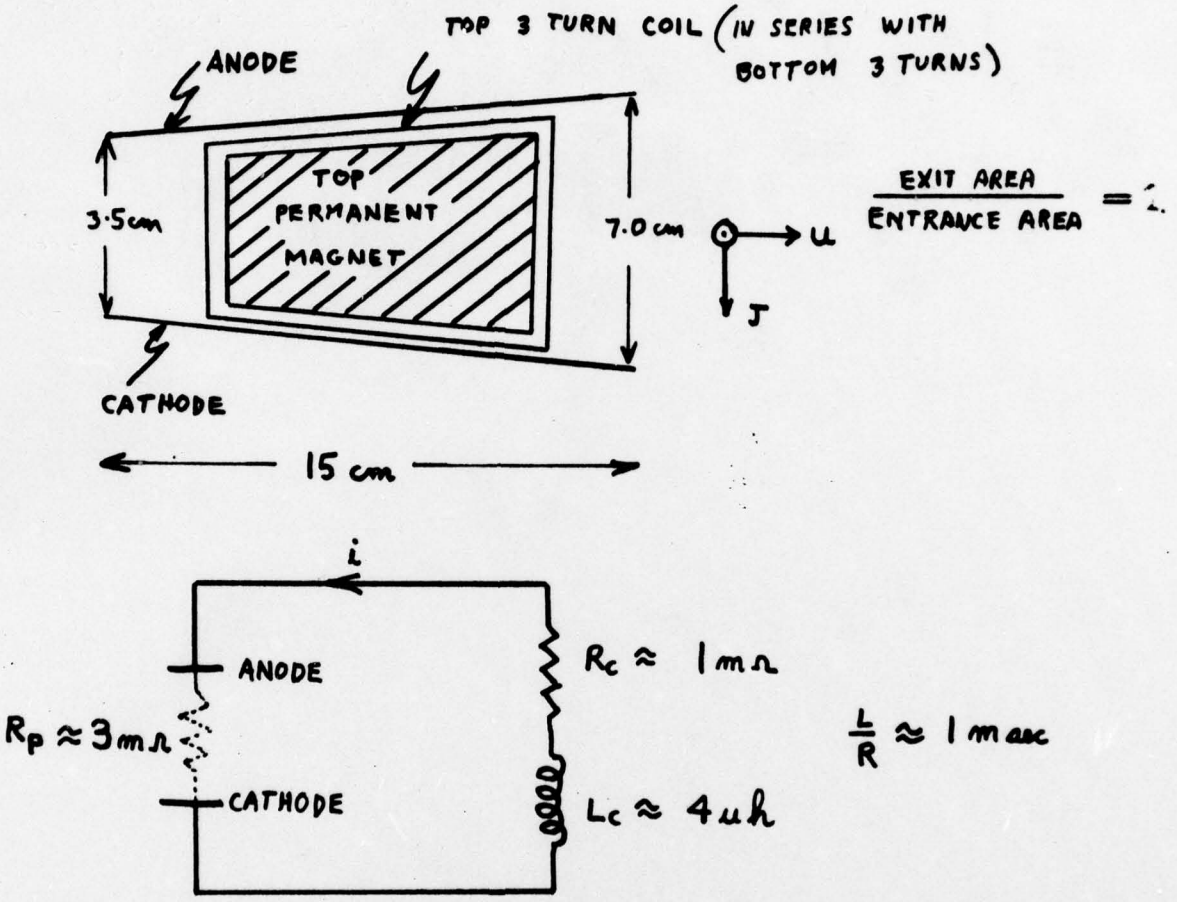

Figure 18. Geometric and electric design parameters for the Ames II Channel.

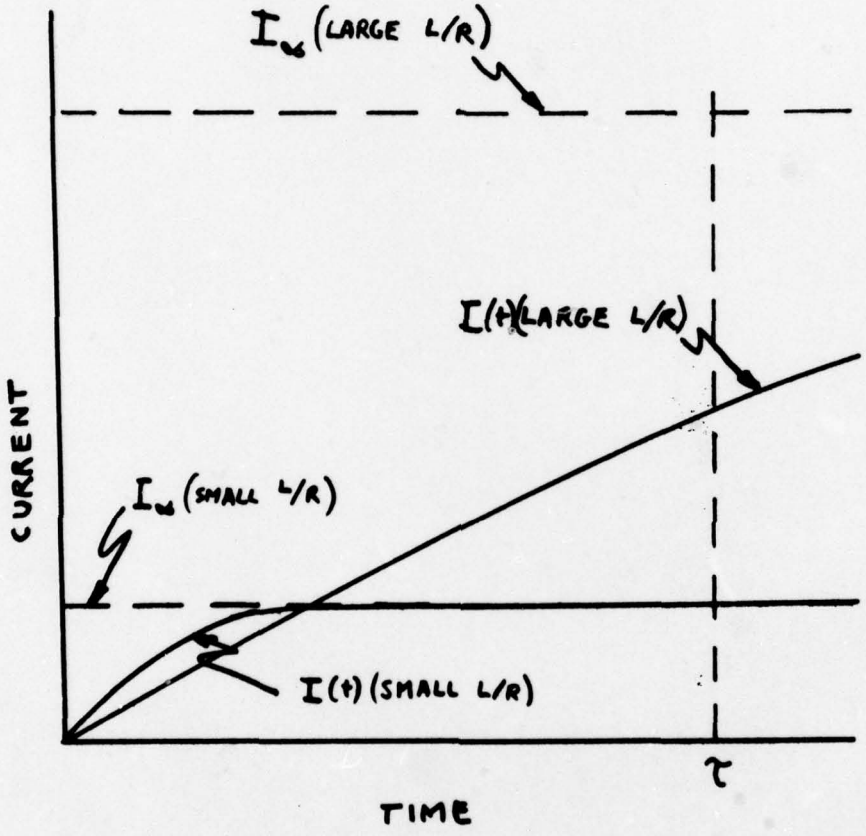

Figure 19. Current versus time for a small and a large L/R.

expected current density j ($> 1000 A/cm^2$) in the channel. This ensures that the flow goes subsonic with the plasma temperature maintained approximately constant throughout the channel. If the plasma resistance is high then j is lowered, the expected decelleration of the flow does not occur, the flow velocity increases and the temperature falls and the plasma electrical conductivity falls even further. It can be seen that any increase in the plasma resistance has a dramatically adverse effect upon the generator performance.

Initial experiments had been done at low voltage with a small capacitor and series resistor attached to the electrodes to give a pulse of current through the plasma.[3] These experiments were mainly to correlate the current pulse with the plasma test-time as the current was not large enough for arc mode operation. To ensure arc operation (several hundred amps through the plasma) a capacitor bank consisting of 40 x 570 μf capacitors was constructed. The capacitor bank was attached to the channel electrodes through various series limiting resistors. The current through the plasma and the voltage across the plasma were measured.

The measurements from some of these runs are shown in Table II (Page 61). The last column is labelled apparent plasma resistance as it includes the voltage loss at the electrodes. The net voltage around the circuit has to have the initial UBD ($\approx$ 12 volts) added to it. The plasma resistance would appear to decrease with current but it probably stays fairly constant. The apparent decrease in plasma resistance is a result of the electrode voltage drop becoming a smaller percentage of the total voltage as the current increases. (An oscillogram of the current on Run 46 is shown in Figure 20). One can not determine the electrode voltage drops without many voltage probes in the plasma but, in any case, for the experiments reported in Table I a total (anode plus cathode) voltage loss of between 7 and 14 volts satisfies all cases. The plasma resistance is $\geq$ 109 milliohms. This is, of course, much too large for high current bootstrap operation of the Ames II channel.

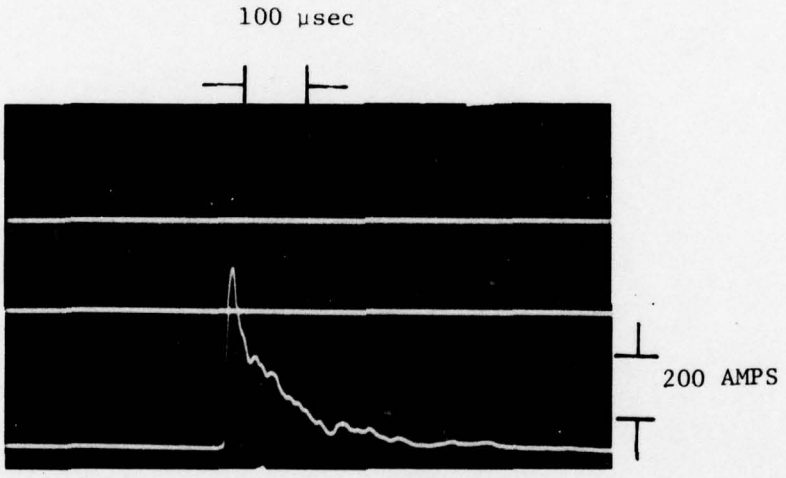

Figure 20. Current through the plasma using a capacitor source.

7.2 Operation of the Ames II Channel as a Pure MHD Generator

The experiments of the previous section showed that the Ames II channel could not be operated in a high current MHD generator mode utilizing only the magnetic field supplied by the permanent magnets (.14 Tesla giving a UB_oD of 12 volts). The maximum current to be expected would be approximately 12 volts/.1Ω = 120 amps at short circuit with no electrode voltage losses. To circumvent this it was decided to operate the generator at higher magnetic fields to get high current data by applying a magnetic field of up to 1.4 Tesla. This was done by supplying the bootstrap coil with current from a capacitor bank. This, of course, precluded bootstrap operation. The capacitor bank was constructed at GE and shipped to Ames. Twelve 170 μf capacitors were used. A photograph of the capacitor bank is shown in Figure 21 and a circuit diagram in Figure 22. As the Litz wire bootstrap coil was designed for low voltage operation the bank voltage was limited to 1.3 kilovolts. The discharge current (at 1.3 KV) was 34 kiloamps which gave a magnetic field of 1.4 Tesla. The 4 μh inductance of the coil results in a fast current rise time (≃100 μsec), the current is crow-barred at its peak and then decays. The low coil inductance also results in a fast decay (≃200 μsec). The fast rise-time and decay of the current meant that the time of peak magnetic field was short. Oscillograms of the bank voltage and current are shown in Figure 23. A slower rise-time and decay would be preferable but this would require a higher inductance coil and this is impossible with the present channel as the coil is imbedded in the channel fiberglass-epoxy structure. The channel was also operated as a simple MHD generator with only the permanent magnetic field. The load resistance was varied at each magnetic field and a load line was thus obtained for each case. The electrical connections for simple MHD generator operation using (a) the permanent magnets only and, (b) with the capacitor bank adding to the permanent magnetic field are shown in Figure 24.

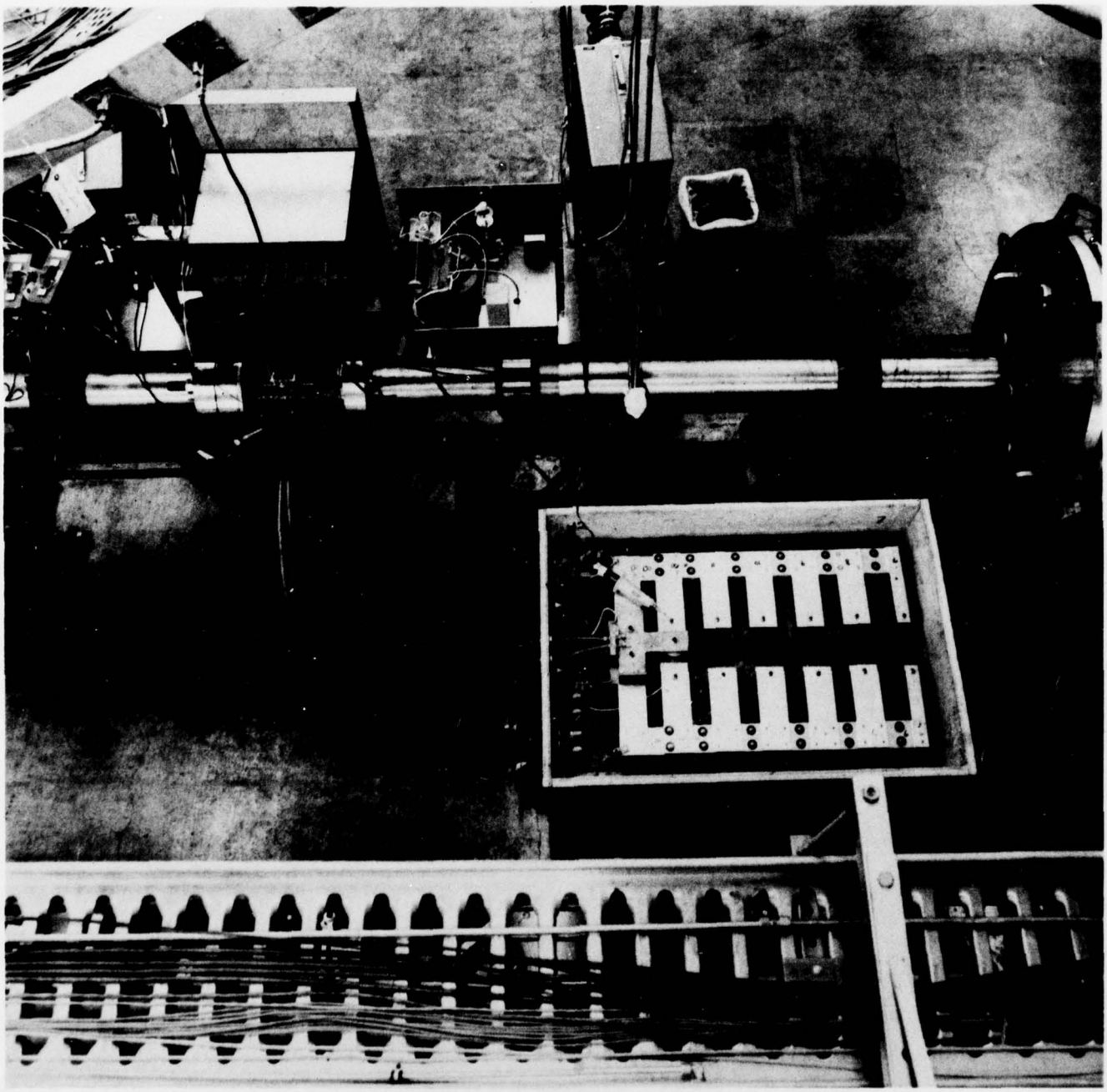

FIGURE 21

OVERALL VIEW OF AMES II MHD CHANNEL INSTALLATION ON AMES ELECTRIC ARC DRIVEN SHOCK TUBE. THE CAPACITOR BANK FOR MAGNETIC FIELD AUGMENTATION IS ALSO SHOWN.

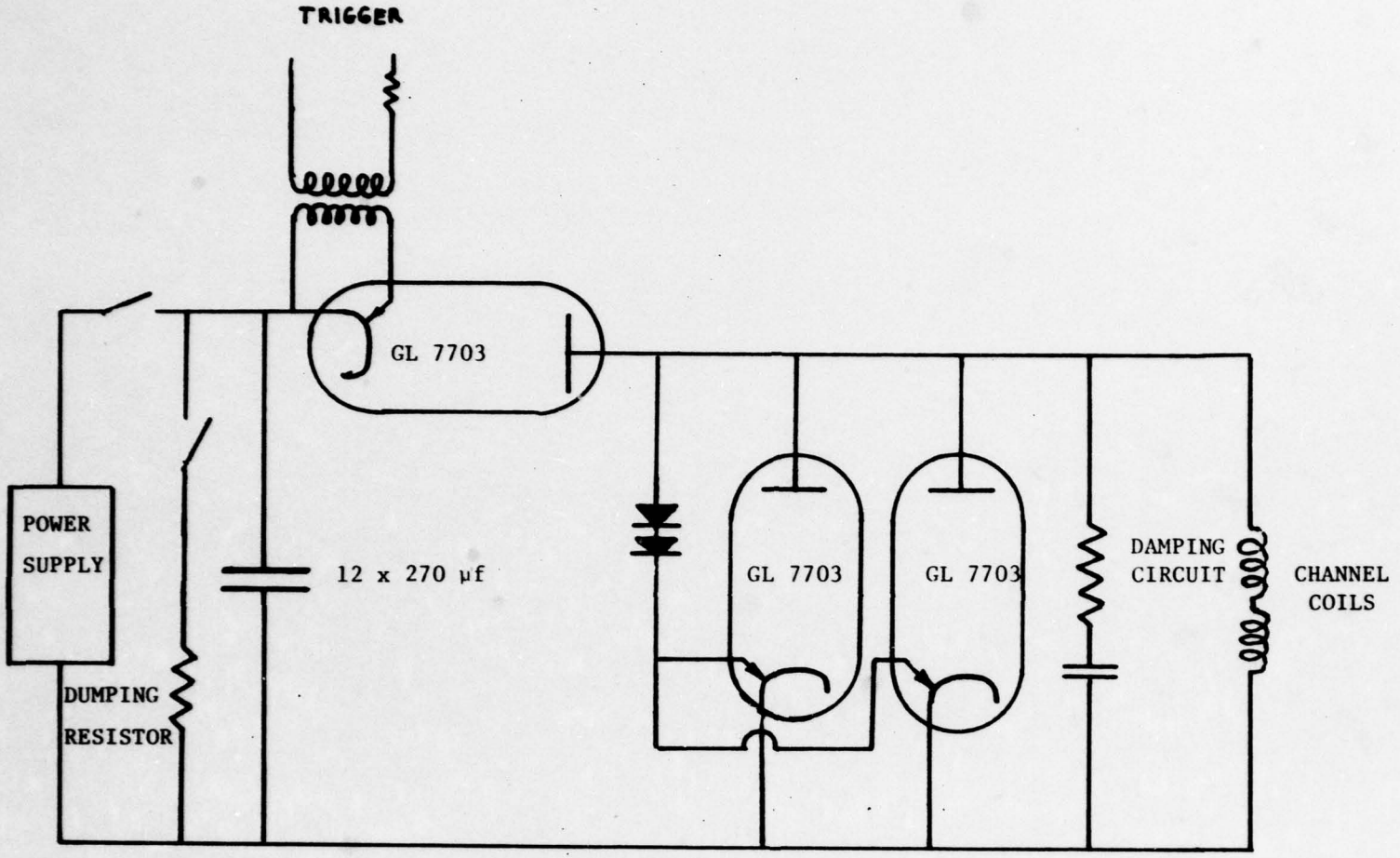

Figure 22. Simplified circuitry of crow-barred capacitor bank used to provide channel coils with current to give a 1.4 Tesla magnetic field.

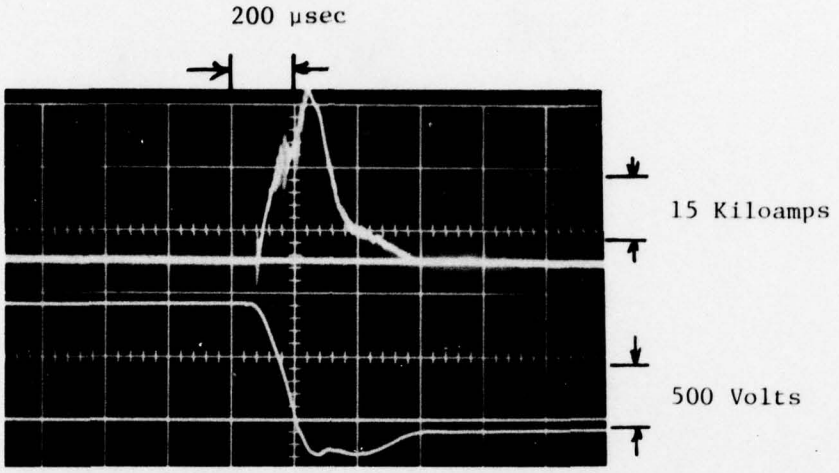

Figure 23. The current and voltage applied to the channel coil to give a large magnetic field.

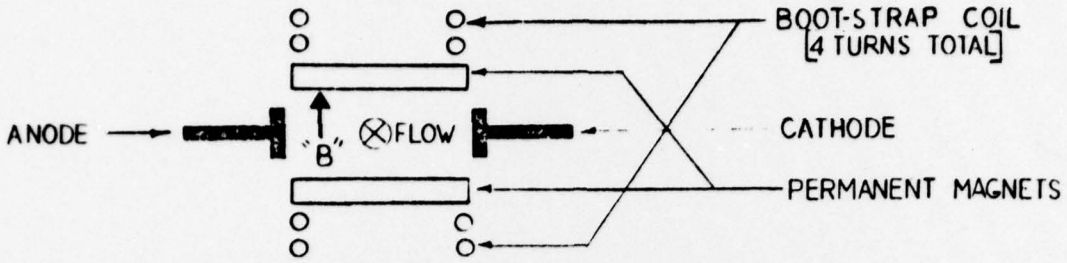

COMPONENT ARRANGEMENT - MHD. GENERATOR

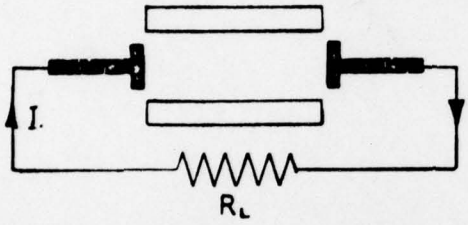

CONFIGURATION 1:- SIMPLE MHD. GENERATOR - "B" FIELD SUPPLIED BY PERMANENT MAGNETS [1.4 TESLA - UBD = 12 VOLTS]

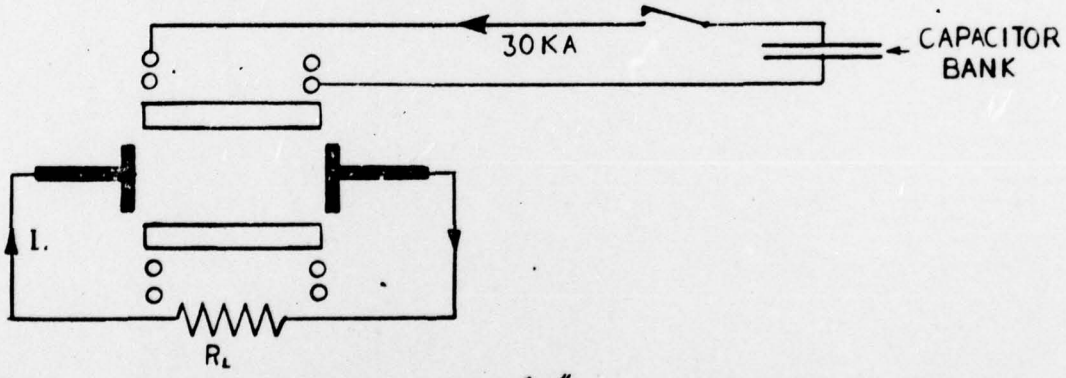

CONFIGURATION 2:- SIMPLE MHD. GENERATOR - "B" FIELD INCREASED BY APPLYING CURRENT TO BOOT-STRAP COIL TO GIVE ~ 1.2 TELSA

Figure 24. Electrical and magnetic configurations for operation of the Ames II Channel as a simple MHD generator.

The initial generator operation, with a permanent magnet only, gave the load line shown in Figure 25. The slope of the load line indicated a generator impedance of 140 mΩ in agreement with the results of the previous section. The dashed portion of the curve cannot be obtained experimentally as one would, at less than 20 amps, be operating in a region of transition between an arc discharge and a glow discharge. As discussed before, a "Delrin" liner was substituted in the driver section for the RTV liner. This resulted in the load line shown in Figure 26. The impedance of the generator was reduced to 70 mΩ. Several other driver pieces were changed but none of them made significant changes in the generator impedance. This result shows that driver gas contamination affects the internal generator impedance.

The current levels were in the tens of amps using the permanent magnet field only and it was obviously desirable to get data at much greater generator current levels. The capacitor bank was used in increase B to as great as 1.4 Tesla. The magnetic field in the channel was measured by firing a shock and measuring the open-circuit UBD voltage and comparing it with the UBD_{oc} obtained using the permanent magnet alone. The calibration curve (UBD_{oc} versus B field) is shown in Figure 27. The maximum UBD voltage available is 122 volts which is an order of magnitude above the electrode losses and also provides high current operation. The generator output current versus UBD_{oc} is shown in Figures 28 and 29. Of utmost importance to the design of future generators is the observation that the generator does not go into a high current mode until the UBD_{oc} voltage reaches the 40→50 volt level. For the conditions pertaining to the EAST shock-tube (as presently configured) this implies that the electrode separation (D) should be increased by a factor of four or the B field (from the permanent magnet) increased by a factor of four or some combination of both in order to achieve the 40 to 50 volts needed for high current operation. At most the electrode separation can be doubled as the internal diameter of the shock-tube is 4 inches. The magnetic field can be

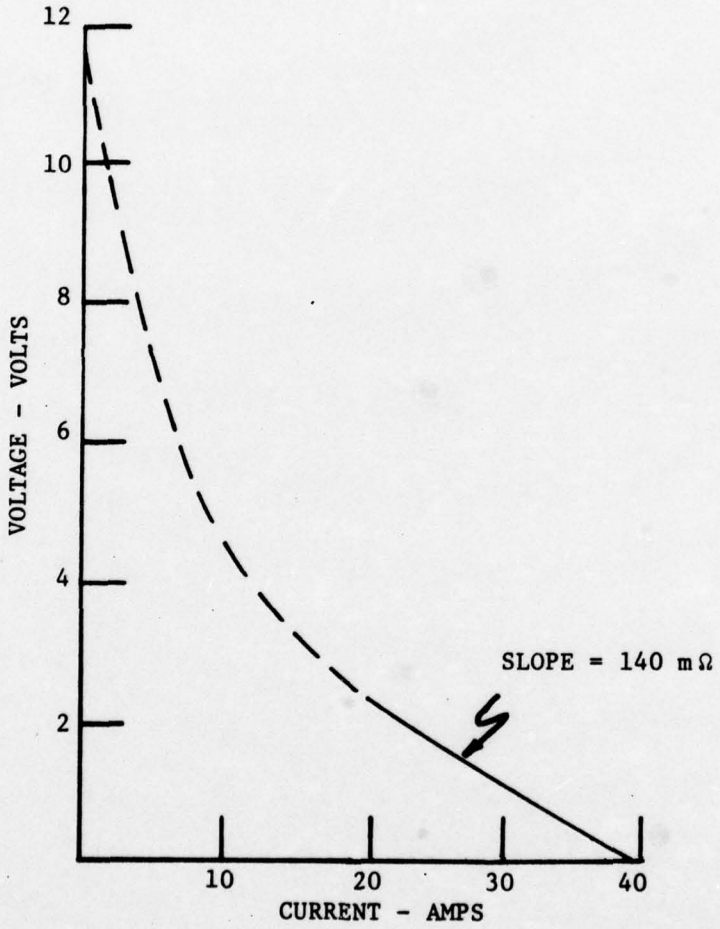

Figure 25. Generator load line before the installation of a "Delrin" liner in the driver.

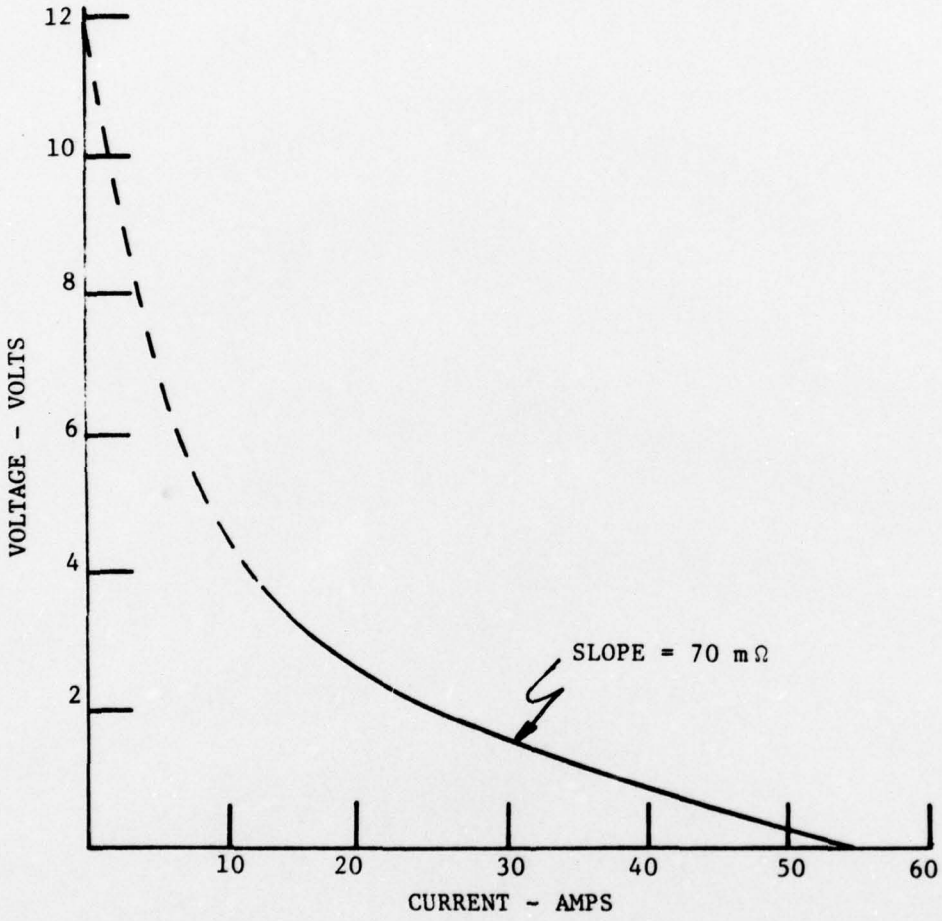

Figure 26. Generator load line after the installation of a "Delrin" liner on the driver. Note driver gas contamination affects the internal plasma impedance (compare with Figure 25).

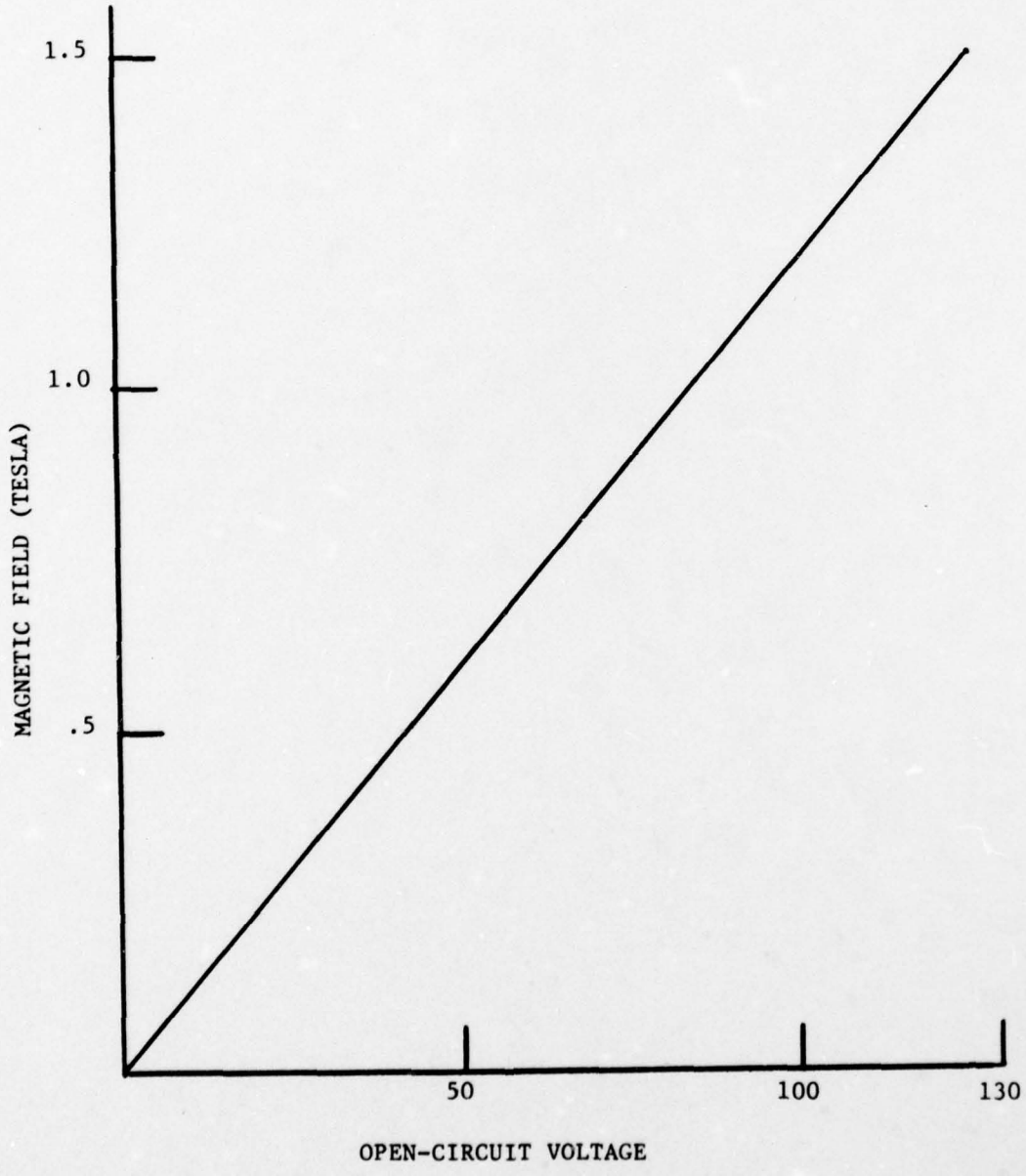

Figure 27. Measured open circuit voltage at various currents applied to the channel coil and the B field obtained.

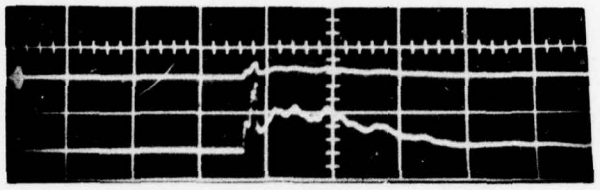

20 A/ V_B = 0

100 A/ UBD = 12V

B = .14T

(a)

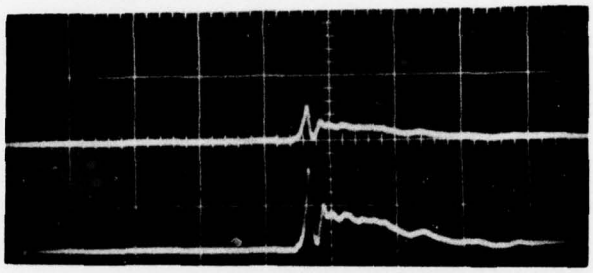

200 A/ V_B = 200

UBD = 30V

80 A/ B = .34T

(b)

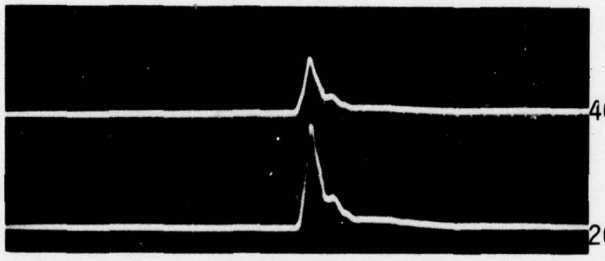

400 A/ V_B = 500V

UBD = 56V

200 A/ B = .64T

(c)

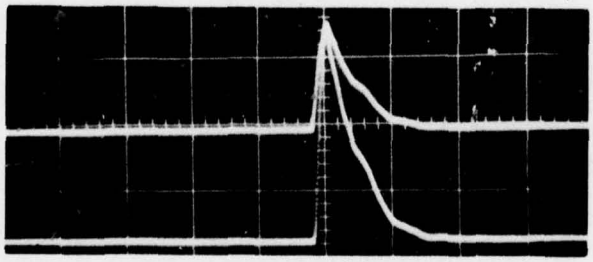

800 A/ V_B = 1.25KV

UBD = 122V

400 A/ B = 1.43T

(d)

Figure 28. AMES II MHD Channel Current Output at various values of UBD_{OC}. Permanent magnet field augmented by a field applied externally.
Case (d) represents a power density of 745 megawatts/metre^3

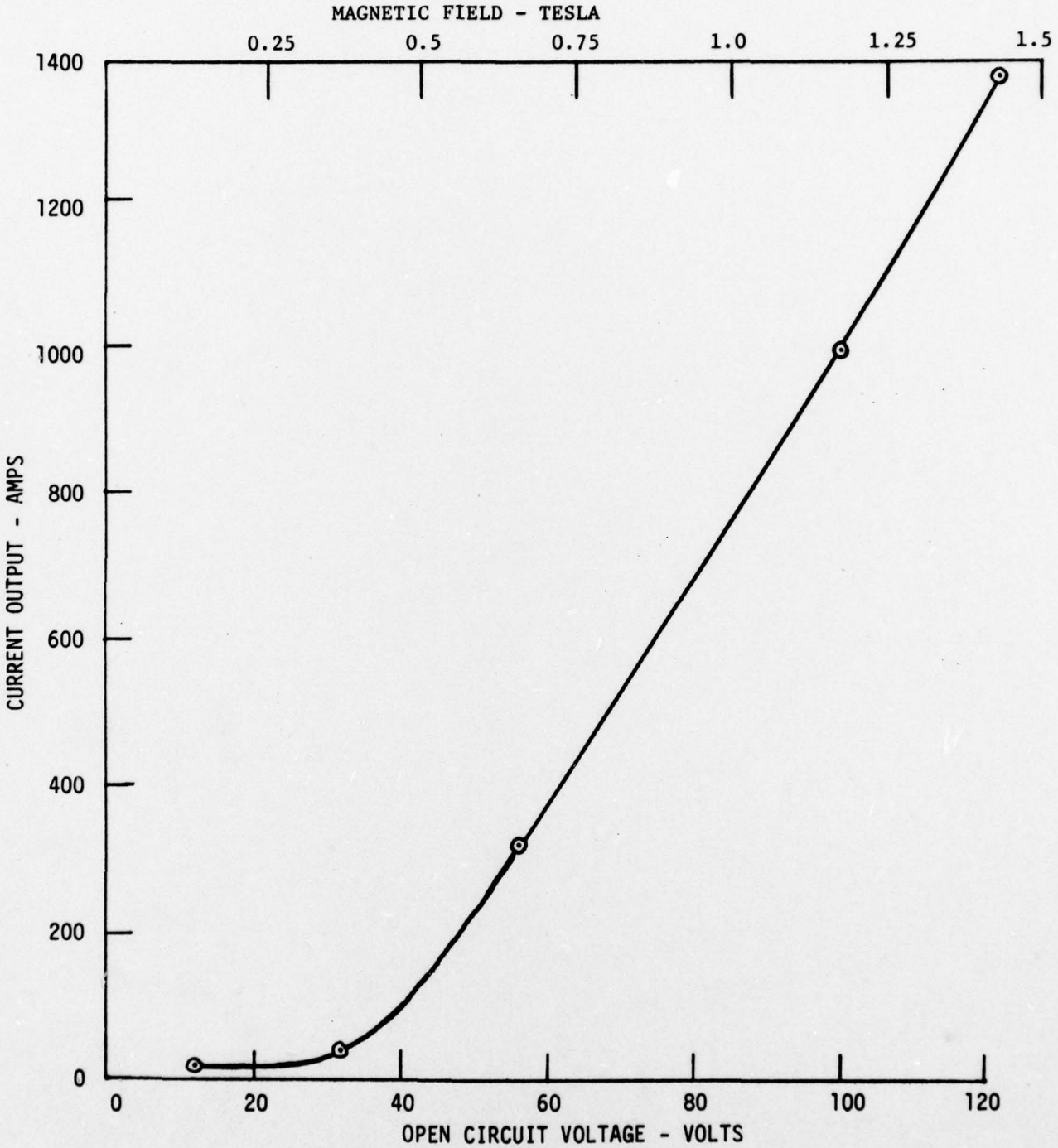

Figure 29. AMES II MHD CHANNEL CURRENT OUTPUT (50 mΩ LOAD) VERSUS OPEN CIRCUIT VOLTAGE. B FIELD SUPPLIED BY CAPACITOR BANK

increased by a factor of two by redesigning its support platform. The UBD_{oc} = 122 volts point gave a peak output current of 1280 amps into a 50 mΩ load or 82 kilowatts. This represented an energy density of 745 megawatts/meter^3.

7.3 Discussion of Open-Circuit UBD Measurements

The open circuit voltage measurements give a good indication of the effect of area ratio and hence temperature drop on the plasma resistance. Figure 30 shows the geometrical and electrical layout for the 2:1 area ratio, flush electrodes. The theoretical UBD_{oc} at the front of channel for .14 Tesla should be 10 volts and for the rear 36.7 volts (Figure 30). The measured UBD_{oc} was 12 volts, i.e. the value at the front of the channel. This is due to the fact that a single electrode pair is used which in effect shorts out the local open circuit voltage along the channel axis and clamps it at its value at the narrow upstream end. Similar behavior is to be expected in any single electrode pair divergent channel in which UBD is not constant, i.e. in a lightly loaded generator. Since our generator was lightly loaded, due to its large internal impedance, it was thus necessary to use a nearly constant area generator to prevent this internal shorting from reducing generator performance.

7.4 Investigation of Various Electrode Surfaces and Channel Area Ratios

The experiments described above were all done using tungsten sprayed copper electrodes and a channel area ratio of 2:1. An investigation of other electrode configurations was done primarily because at the power outputs obtained, the gas accellerated through the channel and hence the gas temperature dropped, which lowered the electrical conductivity. Some of the electrodes had 1 mm tungsten pins inserted into copper surfaces to see if getting the pins (1/8" long) outside

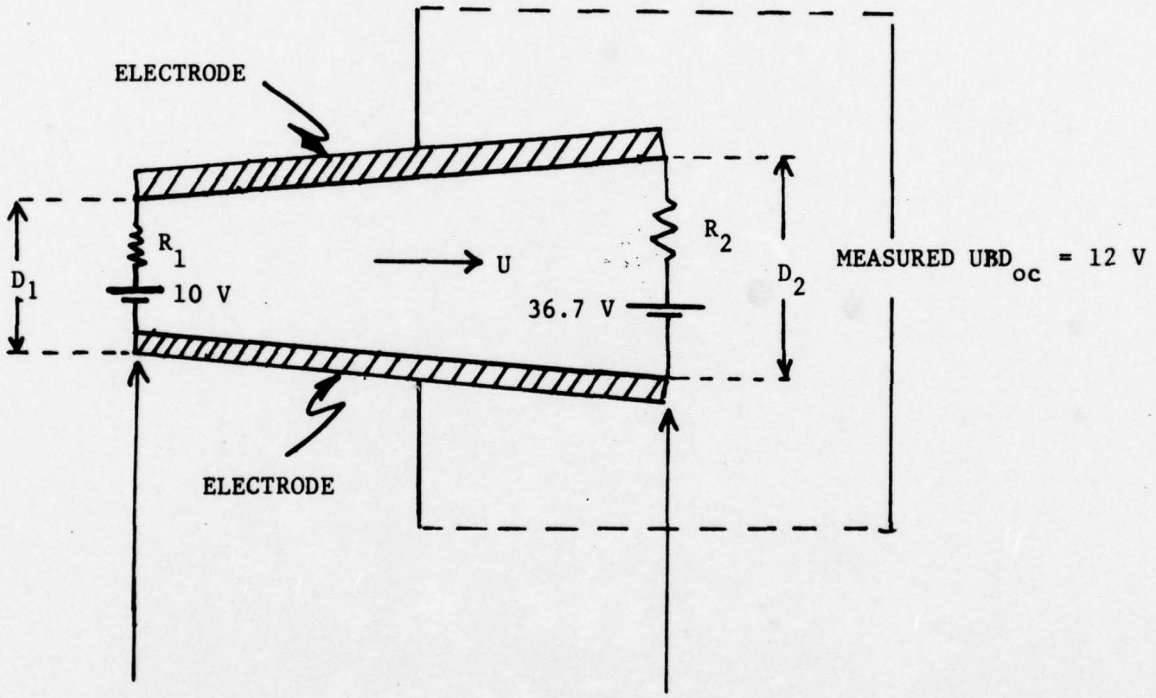

U = 2040 m/sec
D = 0.035 m
B = 0.14 T
UBD_{oc} = 10 V
ΔV_{R_1} = 2 V

U = 3743 m/sec
D = 0.035 m
B = 0.14 T
UBD_{oc} = 36.7 V
ΔV_{R_1} = 24.7 V

$$\frac{R_2}{R_1} = 12.35$$

Figure 30. Geometrical and Electrical Parameters of Ames II Channel to Show Significance of Open Circuit Voltage Measurements

the boundary layer would help the current emission. A photograph of one set of electrodes is shown in Figure 31. The various electrodes tried were as follows:

(a) Tungsten Coated Copper Area Ratio = 2.0:1

(b) Tungsten Pins in Copper Area Ratio = 2.2:1

(c) Tungsten Pins in Copper Area Ratio = 1.4:1

(d) Tungsten Pins in Copper Area Ratio = 1.0:1

A series of runs at various magnetic fields and load resistances were done to characterize the simple MHD generator performance of each of these electrodes. The runs were repeated with the channel at a different shock-tube station. The channel was originally located 34 feet from the driver as this was judged to be the best compromise between shock velocity and test-time. The channel was moved 10 feet nearer the driver to be in a higher Mach number regime but with the expectation of a loss in test-time. The Mach number was higher but no loss in test time occurred. It is thus clear that the driver gas boundary layer is swallowing the test gas. A comparison of the generator outputs in both locations (but otherwise identical conditions) operating in the bootstrap configuration is shown in Figure 32. The increased Mach number resulted in an approximately 15% increase in current but also the current profile was more uniform with time.

Figure 33 is a chart of the current outputs for the various electrodes at both locations. The flush electrodes at very low magnetic fields gave currents of less than 20 amps (Runs 66, 108) whereas the pin electrodes gave as much as 70 amps (Run 98) at low fields (.14 Tesla from the permanent magnets). Conversely the flush electrodes at 1.16 Tesla gave more current (Runs 70, 110) than the nearly identical area ratio pin electrodes (Runs 83, 84, 100). The conclusions are 1) electrode losses are a primary performance factor, and 2) at low fields

the pin electrodes break down easier but at higher fields (hence current levels) the combined effect of the Lorentz force decelleration and gas dynamic friction from the pins reduce the gas velocity and thus the power more than with flat electrodes. Bootstrap operation is at present a low current mode and therefore the pin electrodes work best. Oscillograms of flush electrode bootstrap operation and pin electrode bootstrap operation are shown in Figure 34 for runs 111 and 93. The peak power output was 280 watts for run 93 versus 146 watts output under similar conditions into a 50 mΩ load. The generator added 62 gauss to the initial 1400 gauss so a small increase in magnetic field resulted in a large increase in power output. This key result proves the efficacy of self excited MHD generator operation. The electrical hook-up for bootstrap operation is shown in Figure 35. The current output was measured with a Rogowski coil and an active integrator gated into operation by the output of a pressure transducer located at the reflecting end wall of the channel. The integration time was 10 milliseconds so the gating insured no output until the arrival of the shock. The integrator circuit is shown in Figure 36.

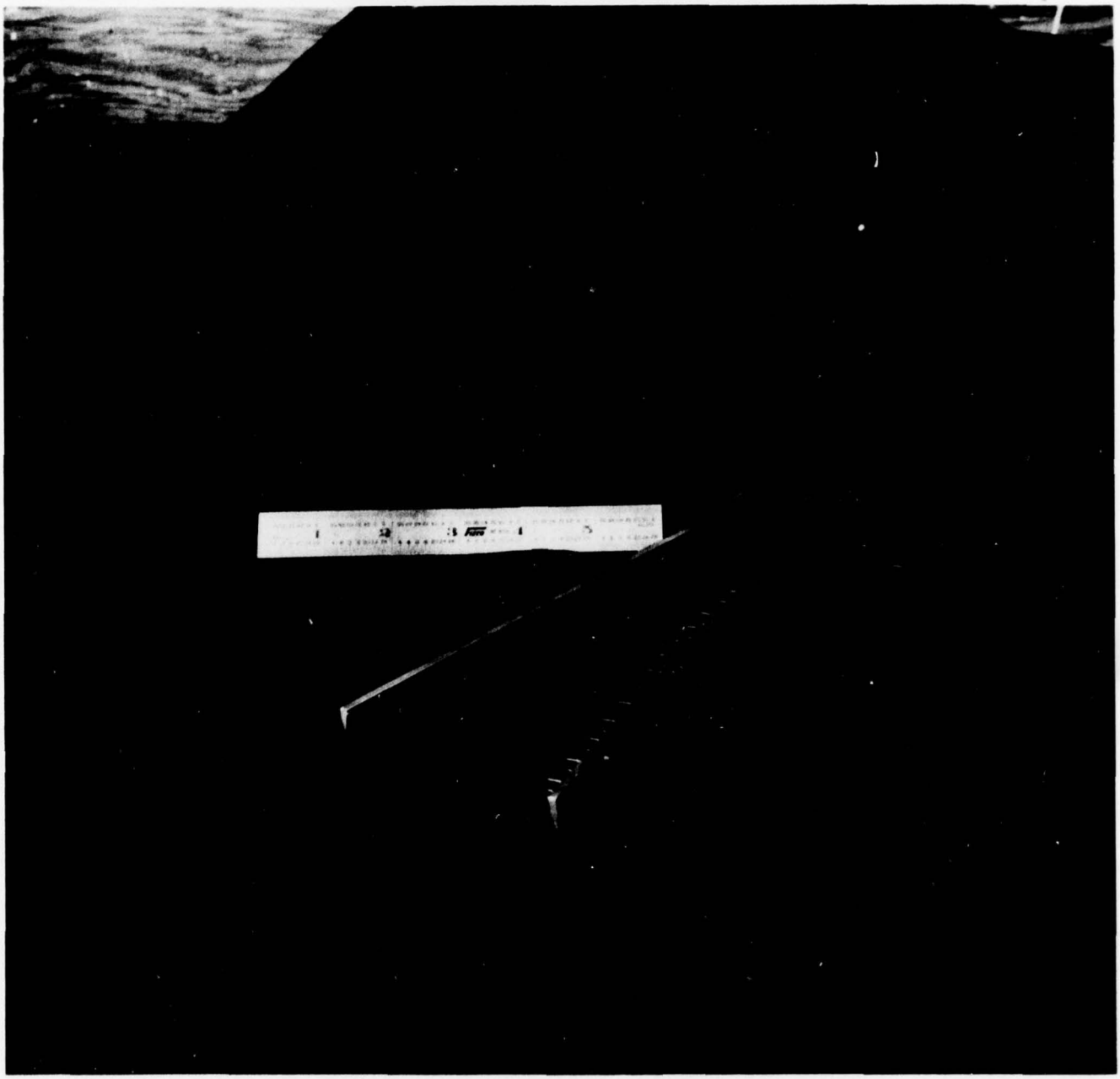

FIGURE 31

AMES II MHD CHANNEL ELECTRODE BLOCKS. TUNGSTEN PINS IN COPPER PLATES.

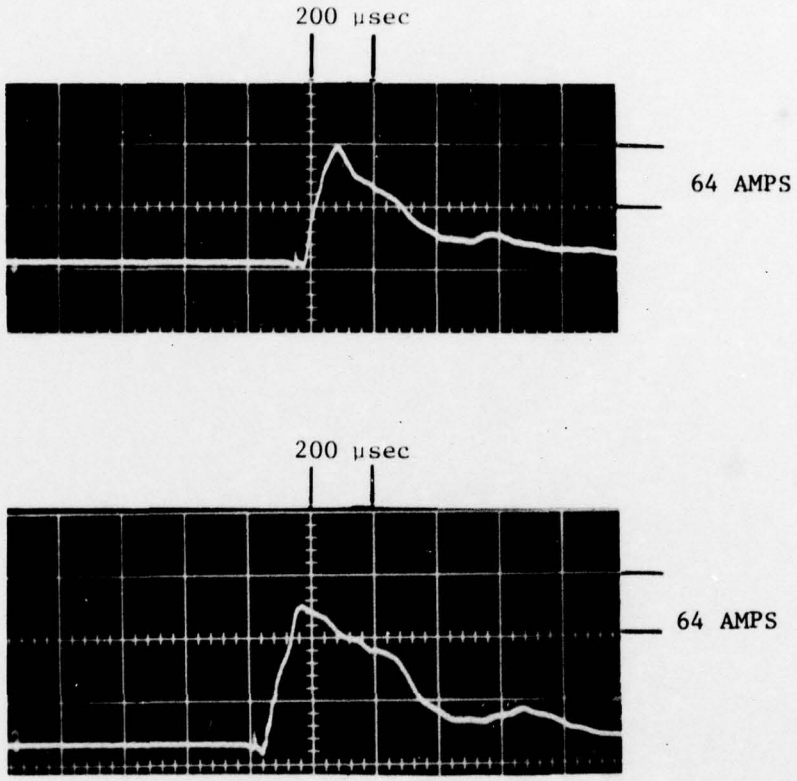

Figure 32. BOOTSTRAP CURRENT OUTPUTS

TOP - GENERATOR 34 FFET FROM DRIVER

BOTTOM - GENERATOR 24 FEET FROM DRIVER

ELECTRODES	2:1F	2:1F	2.22:1P	2.22:1P	1.4:1P	1.4L1P	1:1P	1.4:1F
LOCATION	A	B	A	B	A	B	B	B
CURRENT OUTPUT AT B=.14 TESLA	12A	16A	60A	70A	54A	44A	60A	-
CURRENT OUTPUT AT B=1.16 TESLA	960A	800A	620A	525A	560A	600A	400A	690A
BOOTSTRAPPING	-	30A	-	60A	120A	140A	99A	86A

ELECTRODE NONEMCLATURE - SEE TEXT

LOCATION A - CHANNEL 34 FEET FROM DRIVER

LOCATION B - CHANNEL 24 FEET FROM DRIVER

Figure 33. Chart of the MHD channel current outputs using various electrodes at two different distances from the driver.

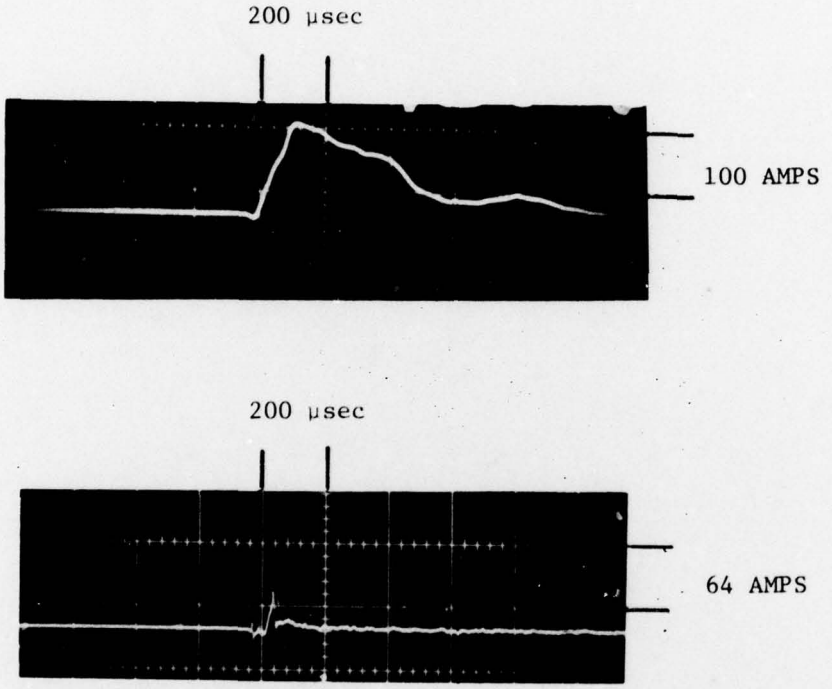

Figure 34. (Top) Bootstrap current using pin electrodes - Run 93

(Bottom) Bootstrap current using flush electrodes - Run 111

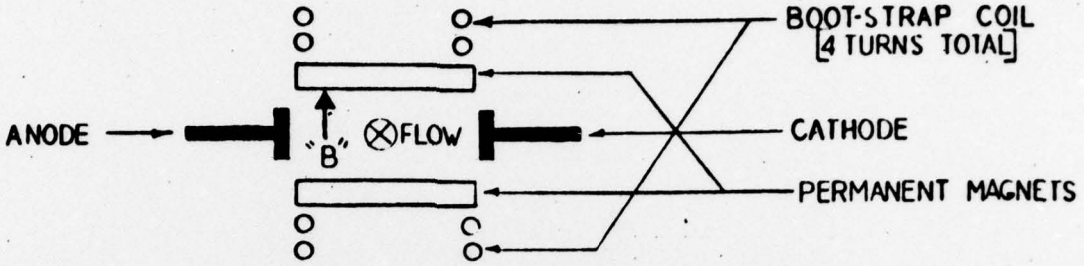

COMPONENT ARRANGEMENT - MHD. GENERATOR

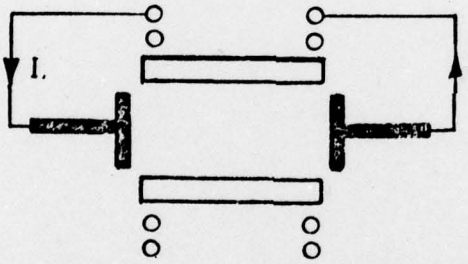

CONFIGURATION 3:- MHD. GENERATOR - OUTPUT APPLIED TO BOOT-STRAP COIL TO INCREASE "B" FIELD

Figure 35. Electrical Connections for Bootstrap Generator Operation

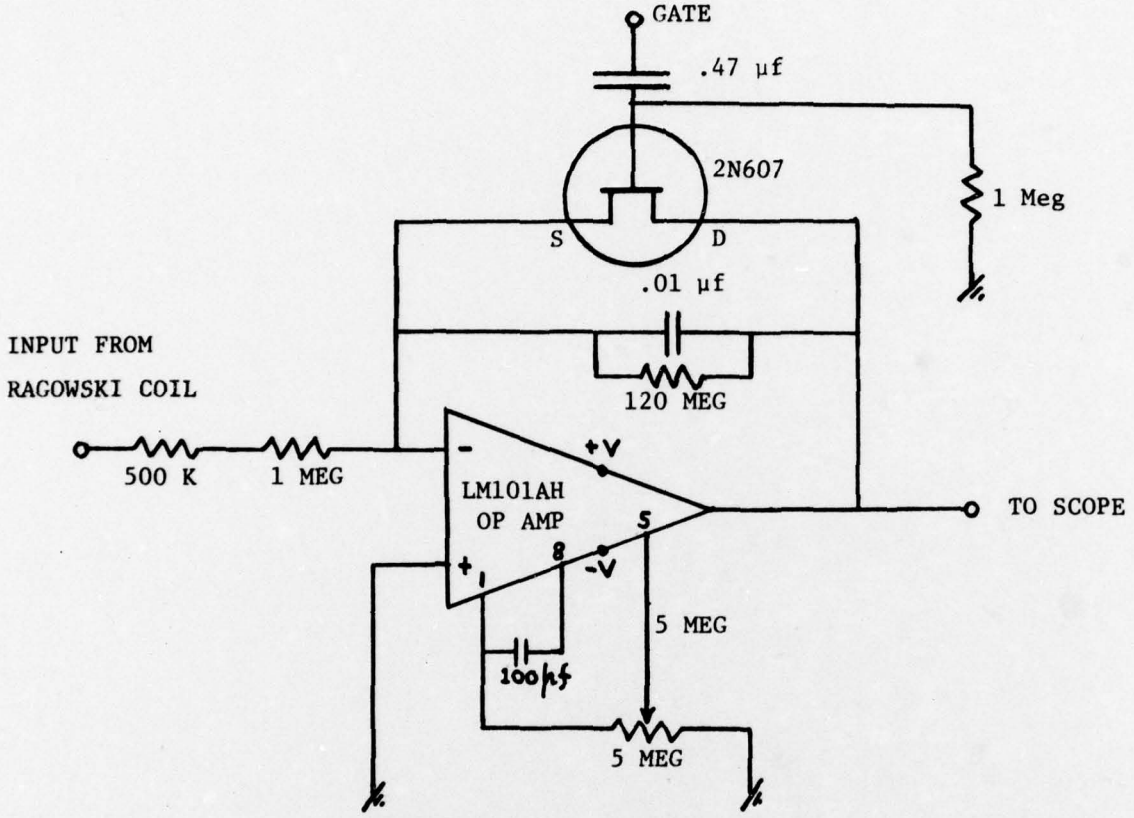

Figure 36. Gated Active Integrator for Rogowski Coil.

TABLE II

RUN	MACH NO.	APPLIED VOLTAGE (VOLTS)	SERIES RESISTANCE (mΩ)	CURRENT (AMPS)	ELECTRODE VOLTAGE	APPARENT PLASMA RESISTANCE (Milliohms)
46	19.6	100	83	580	63.9	109
49	20.1	75	53	444	63.5	142
50	19.3	50	0.8	432	62.5	143
51	19.3	40	5.4	240	50.7	210
52	19.93	30	5.4	276	40.5	146
53	20.6	20	5.4	180	31.0	171
54	19.3	10	5.4	114	21.4	187

SECTION 8

8.0 Experiments on the GE/ONR Shock Tunnel

The previous low magnetic field experiments performed using the GE I channel have been summarized in section 6.4 and Table I. To explore stronger electromagnetic interactions experiments at higher initial magnetic fields were performed. The analysis of these experiments is still in progress. However, as an example of the range of power and energy outputs, 400 joules and 280 kilowatts were obtained at 2.1 Tesla with a 10 mΩ resister in series with the bootstrap coil.

REFERENCES

1. Dannenberg, R.E., "A New Look at Performance Capabilities of Arc Driven Shock Tubes", 11th International Symposium on Shock-Tubes & Waves, University of Washington, Seattle, Washington. July 11-14, 1977.

2. Marston, C.H., Tate, E., Zauderer, B., "MHD Generator Investigations Annual Report", ONR, 1975-6.

3. Marston, C.H., Tate, E., Zauderer, B., "MHD Generator Investigations Annual Report", ONR, 1974-5.

APPENDIX I

GASEOUS METALS COMPOUNDS FOR MHD SEEDING

Argon would appear to be the obvious first choice as a high temperature MHD working fluid. Its transport properties are well known and at a sufficiently high temperature its conductivity is large because of its low electron-atom collision cross-section. However, in practice, to attain and hold the required temperature is not easy. Radiation cooling keeps the temperature at a lower than desired level. In the present experiments it is estimated that the stagnation temperature is less than 13,000°K whereas it would be greater than 18,000°K in the absence of radiation cooling. The electrical conductivity of argon falls very rapidly below 15,000°K.

Explosively derived MHD plasmas would seem to be considerably better in this respect as one can reach the kilobar range in pressure and the radiation energy losses will be a smaller proportion of the total energy in the plasma. However, temperatures of 40,000°K are required to get sufficient electrical conductivity from the products of explosives. As radiation losses increase as the temperature to the fourth power therefore the losses at 40,000°K are sixteen times greater than at 20,000°K. Nevertheless explosives offer the best chance of obtaining the desired electrical conductivity.

To circumvent the radiation cooling problem, given the presently available driver energy from the EAST facility, a working fluid whose electrical conductivity at 13,00°K is similar to that of argon at 18,000°K is desirable. Xenon has alower ionization potential than argon (12.1 eV versus 15.7 eV) and a higher molecular weight so xenon can be driven at a larger Mach number but when expanded through the channel nozzle to supersonic velocity its actual velocity is 1.4 times less than that of argon. Any gain in conductivity is thus offset by a loss in Faraday voltage. Conversely, helium would have a 3.2 times greater velocity through the channel than argon but with a molecular weight of 4 it can not be shock-heated as strongly as argon. Cesium would work well but presents mechanical obstacles. Because of

cesium's low vapor pressure at room temperature, to fill the shock-tube with cesium to a p_1 of 25-75 mm Hg would require heating of the whole shock-tube and channel. This would be a major undertaking.

An alternative to noble gases and cesium would be gasious metal compounds. The metal atoms in these compounds have lower ionization potentials than argon and their volatility at room temperature is such that one can get initial pressures in the shock-tube of 10 to 30 mm Hg.

In general, metal compounds which are relatively volatile at or around room temperature fall into the following categories: (1) metal halides, (2) metal hydrides, (3) organo-metallics, and (4) metal carbonyls.

Typical examples of the metal halides would include BF_3, BCl_3, $TiCl_4$, $SnCl_4$, $SbCl_5$ and WF_6. These materials are in general corrosive, toxic gases which hydrolyse easily in moist air to form the corresponding hydrogen halides.

The metal hydrides include compounds such as B_2H_6, SiH_4, GeH_4, PH_3, etc. These materials are in general quite volatile (BP<0°C), however, they are usually pyrophoric and/or explosive on contact with air and quite toxic.

The organo-metallics are less reactive than the hydrides and are flammable and in some cases pyrophoric. These materials are generally quite toxic. Their volatility is much less than the hydrides. Compounds considered included $Al(Me)_3$, $Sn(Me)_4$, $Pb(ET)_4$, $As(Me)_3$ and $Zn(Me)_2$. These materials are generally expensive.

The carbonyls are the least reactive of the group. However, they are toxic and of moderate volatility. Candidates included $Fe(CO)_5$ and $Ni(CO)_4$.

Several metal compounds are suggested as candidates. These were selected primarily on the basis of the estimated stagnation temperature needed to achieve the same electron concentration as that of argon at 18,000°K and 100 atm. Other considerations such as Mach Number, electron cross-section, channel fueling, cost and handling characteristics were also made.

The selected candidates are:

1) $Fe(CO)_5$ - iron carbonyl I.P. - 7.83

Relatively inert - flammable - toxic

M.W. - 196 T(P = 30 mm) = 28°C

Cost - Modest T(P = 100 mm) = 50°C

Very easily decomposed

Ts ~11,800°K

2) $Al(CH_3)_4$ - aluminum trimethyl I.P. - 5.96

Pyrophoric, may detonate, reacts vigorously with water

M.W. - 72.09 T(P = 30 mm) = 43°C

Primarily dimeric in gas phase T(P = 100 mm) = 69°C

Should not react with shock tube

Cost - Modest

Ts 12,800°K

3) $TiCl_4$ - titanium tetrachloride I.P. - 6.81

Corrosive, hygroscopic liquid, evolves HCl an hydrolysis

M.W. - 190 T(P = 30 mm) = 40°C

May pose a corrosive problem in shock tube T(P = 100 mm) = 71°C

May suffer conductivity loss because of chlorine - electron interactions

Cost - Modest

Ts - 10,300°K

WF_6 - Tungsten Hexafluoride I.P. - 8.10

Corrosive, hygroscopic liquid, hydrolyzes upon contact with moisture to form HF

M.W. - 297.84 B.P. - 17°C

May pose a corrosion problem in shock tube

Fluorine - electron interaction may be a problem

Cost - Modest

Ts - 12,300°K

Although the ionization potentials of these compounds are lower than that of argon (thus giving larger electron densities at equivalent temperatures) their conductivities are not obviously better. They have larger electron-atom collision cross sections than argon which will affect the gain in electron density. Their conductivities would have to be calculated using available data on cross-sections, etc.

The choice of a metal compound (apart from the criteria mentioned previously) would be determined by several other factors as well as electrical conductivity. If one uses iron carbonyl as an example, it has a molecular weight of 196 so has an advantage over argon (MW=40) of 2.2 times in initial shock Mach number so a higher T_2 can be reached. This advantage is partially offset by iron carbonyl's decomposed molecular weight of 17.8 which means the reflected shock processes a lower molecular weight fluid so T_5 is lowered. Upon expansion through the channel nozzle the decomposed iron carbonyl again has an advantage over argon as its sound velocity is 1.5 times greater so a larger Faraday voltage is developed.

APPENDIX II

PRIMARY DESIGN OF A PLASMA ELECTRICAL CONDUCTIVITY PROBE

The method chosen for measuring plasma conductivities is one which measures the change in inductance of a coil when a plasma passes through it (or is contained by it). The method is in principle simple but in the past has been in practice extremely difficult to design, calibrate and use. The advent of large scale integrated circuits has simplified the method considerably. A block diagram of the concept is as follows:

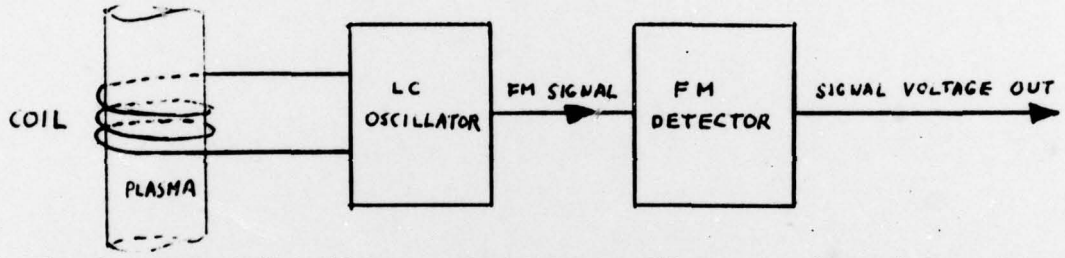

The frequency of oscillation of the LC oscillator is changed from its steady rate when the permeability of the coil is changed by the presence of an electrically conductive plasma. This FM signal is changed to a voltage variation by the FM detector and is recorded. Prior calibration of the coil (by inserting samples of known conductivity) relates the voltage out to the conductivity. This method has been little used in the past as the FM detector had to be constructed from discrete components (tubes, transmitors, etc.) and transformers were only available for discrete frequencies (10.7 MC FM broadcast, 4.5 MC television sound, 455 KC AM broadcast). The design, construction and alignment of such a detector takes about 3 months and one still only had one frequency of operation. This single operating frequency complicates the calibration procedure as samples of conductivity of say 1000 mhos/metre are not readily available (only semiconductors give this sort of conductivity).

The change in inductance is proportional to $f\sigma$ and therefore to calibrate for 1000 mhos/metre one calibrates using a sample with a conductivity of 100 mhos/metre (electrolytic solutions give conductivities of this order but at ten times the frequency. The detector frequency can not be changed so a completely separate electronics circuit has to be fabricated for calibration - this is obviously tedious, indirect and thus subject to error. The method calls for precision but discrete FM detectors are subject to many drift errors. The advent of the Phase Locked Loop (PLL) has changed all this. A PLL such as the 565 costs fifty cents, requires no alignment and only the addition of four external components (plus a small battery) to be operative. A complete mapping of its electrical characteristics can be done in a day. Its frequency of operation can be at any point in the range of .001 cps to 500 Kc and can be set by simply changing the setting of an external potentiometer. Its drift errors are negligible (e.g. 100 ppm/^{o}C at 50 Kc). A circuit diagram of the oscillator, PPL and output amplifier is shown in Figure 37. This circuit has already been constructed in breadboard form and is presently being optimized. The oscillator is followed by an emitter-follower stage to provide isolation from the output cable. The PPL output is filtered to remove harmonics of the operating frequency and the LF356 OP-AMP provides a quiesent voltage output of zero volts. An important advantage of this method is that the same electronics can be used on many experiments. For instance, a Lin Coil (or whatever) fabricated around a two inch shock-tube would not work on a six inch shock-tube - a complete new coil would have to be fabricated. In the case of the PLL method a new coil (several turns of fine wire) is wrapped around the shock-tube, the PLL potentiometer is adjusted to match the new oscillator frequency and the probe is ready to use.

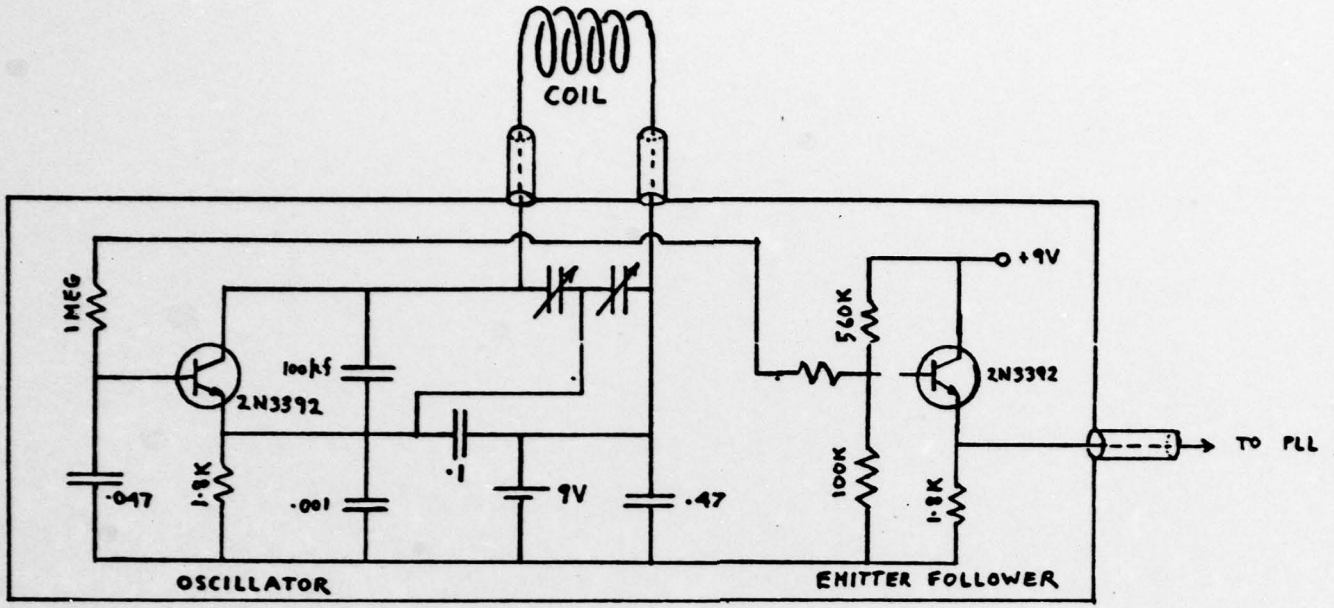

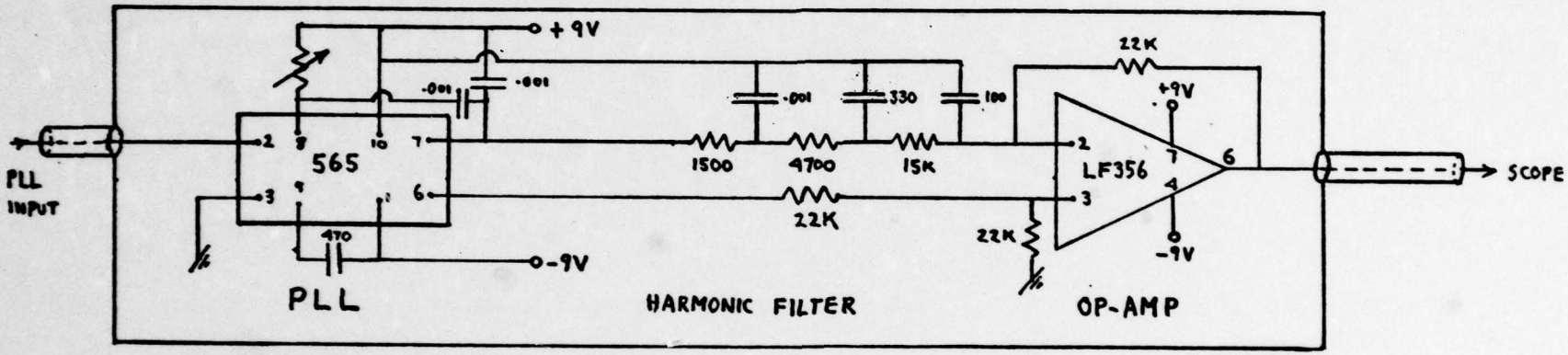

Figure 37. FM Conductivity Probe Circuit Diagram.